Design, synthesis and biological evaluation of novel SARS-CoV-2 3CL^{pro} covalent inhibitors.

Julia Stille,[#] Jevgenijs Tjutrins,[#] Guanyu Wang,[#] Felipe A. Venegas,[#] Christopher Hennecker, Andres Mauricio Rueda, Caitlin E. Miron, Sharon Pinus, Anne Labarre, Jessica Plescia, Mihai Burai Patrascu, Danielle Vlaho, Mitchell Huot, Anthony K. Mittermaier and Nicolas Moitessier**

Department of Chemistry, McGill University,
801 Sherbrooke St W, Montreal, QC, Canada H3A 0B8.

*corresponding authors: nicolas.moitessier@mcgill.ca; anthony.mittermaier@mcgill.ca

[#] These authors contributed equally to this work.

Abstract

Severe diseases such as the ongoing COVID-19 pandemic, as well as the previous SARS and MERS outbreaks, are the result of coronavirus infections and have demonstrated the urgent need for antiviral drugs to combat these deadly viruses. Due to its essential role in viral replication and function, 3CL^{pro} has been identified as a promising target for the development of antiviral drugs. Previously reported SARS-CoV 3CL^{pro} non-covalent inhibitors were used as a starting point for the development of covalent inhibitors of SARS-CoV-2 3CL^{pro}. We report herein our efforts in design and synthesis which led to submicromolar covalent inhibitors when the enzymatic activity of the viral protease was used as a screening platform.

Introduction

Coronaviruses. Coronaviruses (CoV) are a large family of viruses associated with the common cold, as well as far more serious diseases including Severe Acute Respiratory Syndrome (SARS, caused by SARS-CoV infection), which made headlines worldwide in 2002-2003 with over 700 deaths including 43 in Canada,[1] and the Middle East Respiratory Syndrome (MERS, caused by MERS-CoV infection), which was reported in Saudi Arabia in 2012 and killed over 900.[2] The current 2019-2020 outbreak of novel coronavirus (COVID-19, caused by SARS-CoV-2 infection) and the discovery of animal reservoirs provide significant motivation for the development of potent therapeutics against these viruses to prevent future outbreaks.[3,4]

SARS, MERS, and COVID-19 are respiratory illnesses characterized by fever, cough, and shortness of breath, posing significant danger to patients. The fatality rates for those infected with SARS-CoV and MERS-CoV are estimated at about 10% and 35%, respectively.[1,2] Early estimates for SARS-CoV-2 are on the order of 0.5 to 4%, although this number could change substantially as more accurate information on the numbers of infections and deaths becomes available.[5] In contrast to SARS and MERS, COVID-19 has rapidly spread worldwide despite the severe restrictions imposed in many countries, and the number of deaths now exceeds 1 million.[6]

Coronavirus (CoV) and 3-Chymotrypsin-like Protease Inhibition. These viruses express 3-chymotrypsin-like cysteine proteases (3CL^{pro}), also referred to as the main proteases (Mpro) or Nsp5 (non-structural protein 5), which feature a Cys-His catalytic dyad (Cys^{145}, His^{163}) and is required for viral replication and infection. 3CL^{pro} enzymes were identified early on as attractive targets for antiviral development, resulting in several inhibitors and structures of SARS-3CL^{pro}-inhibitor complexes (eg, PDB codes: 4TWY, 2ZU5, 2ALV). The 3CL^{pro} enzymes from SARS-CoV and SARS-CoV-2 share a 96% identity,[7] suggesting that many of the lessons learned for developing SARS therapeutics can be applied to COVID-19. As a note, 3CL^{pro} is not limited to coronaviruses but is also a drug target for the development of antivirals against noroviruses (such as the one involved in gastroenteritis[8]) or antivirals against enteroviruses (eg, antiviral drug 3CLpro-1[9] targeting the hand, foot, and mouth disease enterovirus 71 and **Rupintrivir** originally developed to fight rhoniviruses[10]).

Covalent Inhibitors. The quest for novel antivirals against SARS-CoV and, more recently, SARS-CoV-2 has been intense, and several viral enzyme inhibitors and crystal structures of enzyme-inhibitor complexes have been reported (eg, PDB codes: 6M2N, 6XQU, 6WQF).[11] The presence of a catalytic

cysteine residue in the active site makes 3CL^{pro} amenable to covalent inhibition, a strategy that was successfully employed following the SARS-CoV pandemic (SARS). In fact, many of the reported SARS-CoV inhibitors feature a reactive group, such as an α-ketoamide, epoxide, aziridine, α,β-unsaturated ester (Michael acceptor), or α-fluoroketone, which forms a covalent bond with the catalytic cysteine residue (Cys^{145}), as confirmed by X-ray crystallography (e.g., PDB code: 5N19).[11] Fortunately, a crystal structure of the SARS-CoV-2 3CL^{pro} with a covalent peptidic inhibitor bound to cysteine residue (Cys^{145}), was quickly elucidated (PDB code: 6LU7), followed by many others. This pseudo-peptidic inhibitor, an analogue of **Rupintrivir** (tested on SARS[12] and COVID-19[13]), has been the starting point for a number of drug discovery campaigns.[14-17] Recently, a 3CL^{pro} inhibitor (**PF-0730814**, Figure 1) entered Phase 1 clinical trials.[16] Smaller)ie, more drug-like) inhibitors of SARS 3CL^{pro} (**Rupintrivir** has a molecular weight of 599), such as **2** and **3,** have been devised and it is likely that smaller inhibitors may be discovered for SARS-CoV-2 3CL^{pro} (Figure 1).

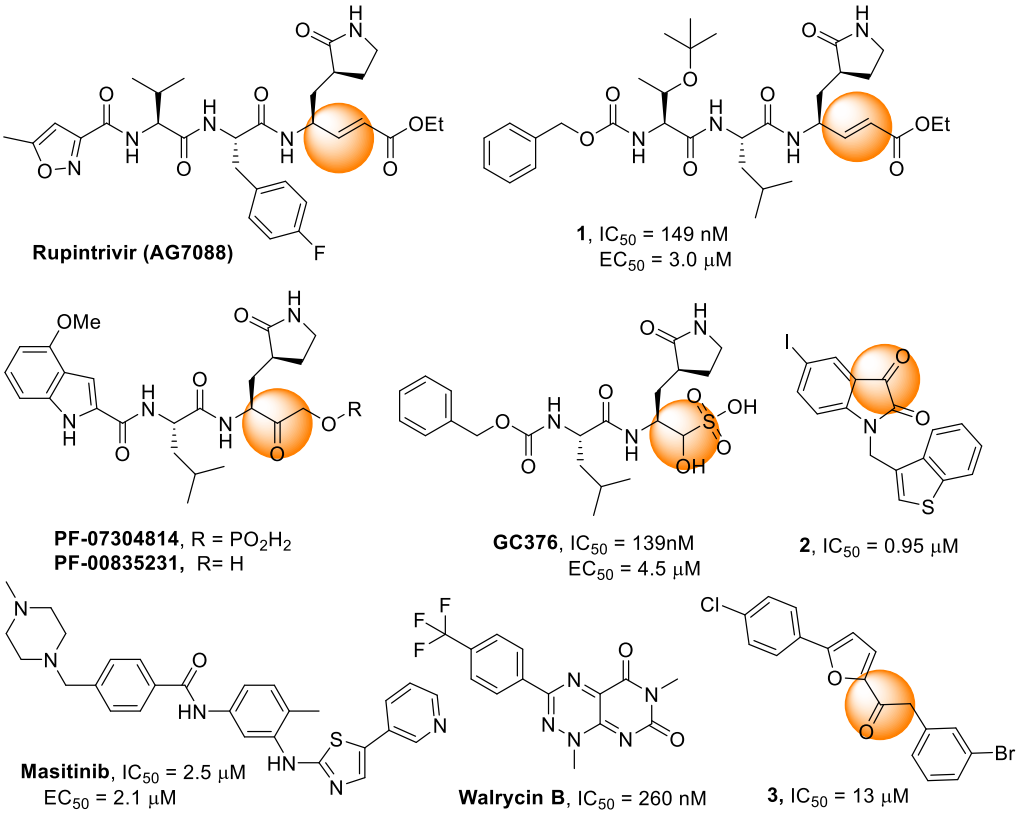

Figure 1. Reported covalent SARS-CoV-2 3CL^{pro} inhibitors **1, GC376**[15] and **PF-0730814**,[18] reported non-covalent inhibitors **Masitinib**[19] and **Walcyrin B**.[20] Reported inhibitors of SARS-CoV 3CL^{pro} **2**[21] and **3**.[22] Orange spheres indicate the warheads for covalent binding.

As described in our recent review,[23] covalent drugs can be extremely effective and useful pharmaceuticals, yet they have been largely ignored in most drug design endeavours and particularly in those concerning structure-based drug design. Concerns about their potential off-target reactivity and toxicity have often been raised.[24] Despite these concerns, there are many examples of covalent drugs on the market, including two of the ten most widely prescribed medications in the U.S. as well as several other common drugs like aspirin and penicillin.[23] The advantages of covalent drugs are becoming increasingly recognized: they have extremely high potencies, long residence times (slow off-rates), and high levels of specificity.[25] Although skepticism persists, many pharmaceutical companies are embracing covalent drugs as exemplified by **Neratinib** (Pfizer), **ZGN-433** (Zafgen) and Afatinib.

3CL^{pro} inhibitor design. Many of the structure-based studies related to COVID-19 to date have employed virtual screening and machine learning techniques. Several ***potential*** 3CL^{pro} inhibitors have been identified, however experimental verification has lagged behind.[26-28] As of today, much of the research has focused on peptidic substrate-like inhibitors (Figure 1). There is currently a need for the development of drug-like inhibitors with synthetically accessible scaffolds that will allow for more thorough investigations of structure-activity relationships. We thought to benefit from our team's expertise in covalent inhibition and from our software that enables automated docking and virtual screening of covalent inhibitors, which is not possible with most commercial packages. We present herein our efforts towards the development of novel potent covalent inhibitors of 3CL^{pro}.

Chemistry

Inhibitor design through covalent docking. In the past years, we have successfully applied covalent docking to the design and discovery of prolyl oligopeptidase inhibitors[29,30] and thought to apply a similar strategy to develop SARS-CoV-2 3CL^{pro} inhibitors. An investigation of the crystal structure of a non-covalent inhibitor bound to 3CL^{pro} of SARS-CoV-2 (PDB code: 6W63) suggested that it might be possible to modify this inhibitor by incorporating a covalent warhead in proximity to the catalytic cysteine residue. As shown in Figure 2, the sulphur atom of Cys^{145} is positioned at 3.2Å (van der Waals distance) from the imidazole moiety. Thus, replacement of the imidazole with a covalent warhead appeared to be a promising strategy to improve the inhibitory potency of this non-covalent inhibitor. Additionally, this scaffold could be prepared via a 4-component Ugi reaction,[31] enabling a combinatorial approach that would provide an efficient synthetic method for preparing diverse analogues. This would provide a significant advantage in exploring structure-activity relationships when compared to

previously reported inhibitors, as a wide range of covalent warheads could be readily incorporated into the same inhibitor scaffold.

It should however be noted that the basic imidazole nitrogen of the original inhibitor interacts with the Gly^{143} backbone amide, an interaction also observed with the furan ring of ML188 (PDB code: 3V3M) or other heterocycles of the same chemical series.[31,32] This Gly amide together with Ser^{144} form the oxyanion hole that contributes to the catalytic activity of this enzyme. In addition, a water molecule (HOH518) interacts with the inhibitor imidazole and the catalytic His^{41}. However, as this water is in a hydrophobic pocket (Val^{42}, Thr^{25}, Leu^{27}), removing this interaction with the water molecule may be detrimental to the free energy of binding. A water molecule in the same location is observed with ML188 (PDB code: 3V3M) although not interacting with the inhibitor and with some of the pseudo peptidic inhibitors such as in structure PDB code: 6Y2G.

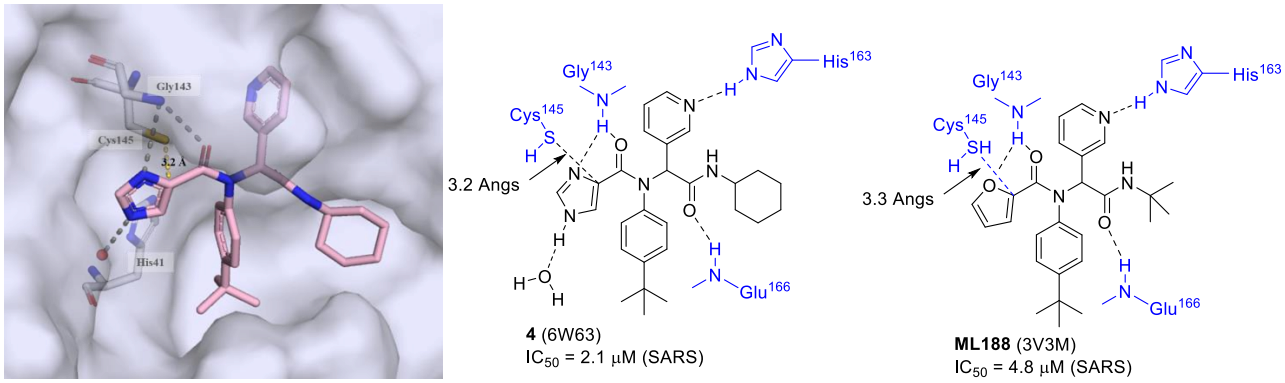

Figure 2. Imidazole of **4** inhibitor and **ML188** interacting with HOH-518 (PDB codes: 6W63 and 3V3M).

In order to validate the design strategy, a virtual library of modified inhibitors was prepared based on incorporation of covalent warheads that could be accessed via a traditional or modified Ugi reaction. These compounds were docked to 3CL^{pro} (using PDB code 6W63) using our docking program, FITTED[33] (Figures 3 and 4). The docked poses (Figure 4) suggested that many of these modified inhibitors would be able to maintain the same non-covalent interactions as the original non-covalent inhibitor while also positioning the warhead close enough to Cys^{145} to facilitate the formation of a covalent bond. While β-lactams and nitriles are well-established covalent warheads, their synthesis via modified Ugi reactions would result in analogues without the *tert*-butyl phenyl group. The formation of a covalent bond may not be enough to overcome the loss of this non-covalent interaction, as is suggested by a decreased docking score. Based on the promising docking results with multiple warheads, a small library of analogues was synthesized for experimental testing.

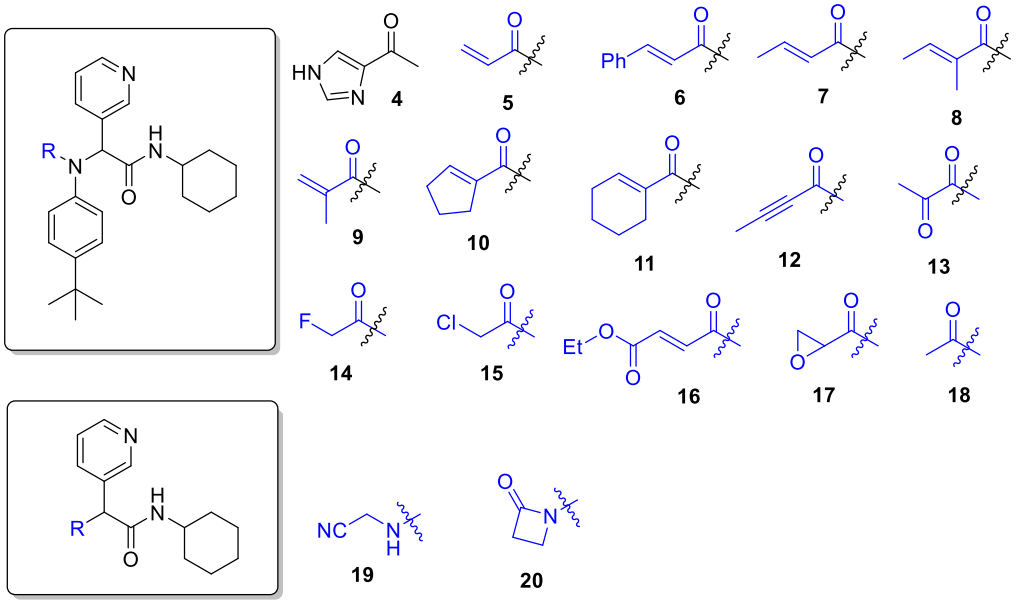

Figure 3. Selected covalent 3CL^{pro} inhibitors for synthesis. **4** is the original non-covalent lead compound.

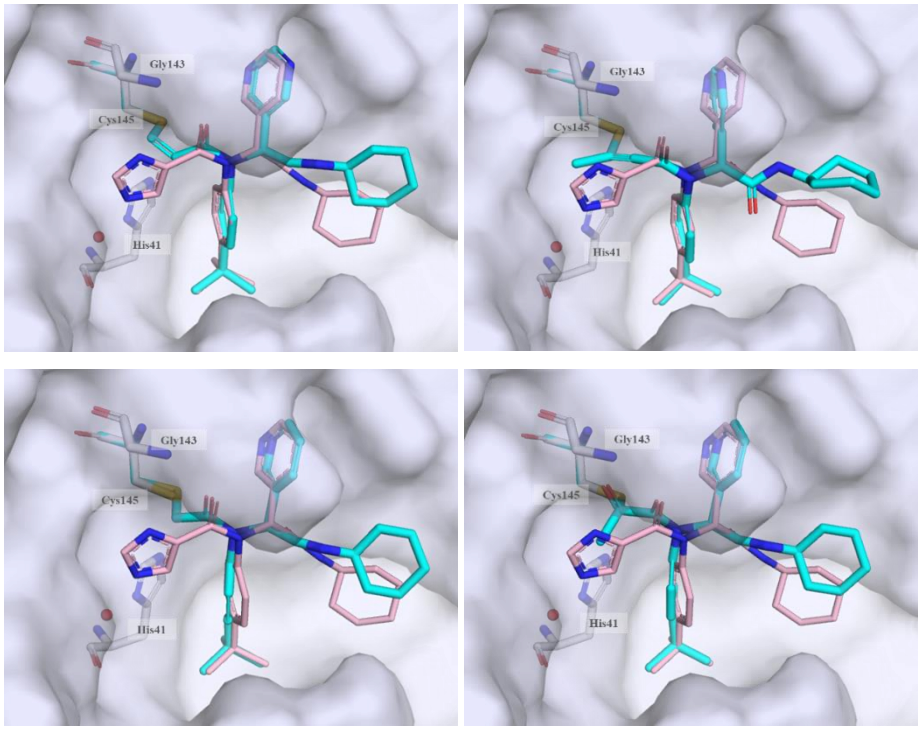

Figure 4. Selected docked binding modes of design covalent inhibitors (cyan) overlaid with the non-covalent inhibitor (co-crystallized) **4** (light pink). Top left: **5**, top right: **12**, bottom left: **15** and bottom right: **13**.

Synthesis. Following a protocol reported by Jacobs *et al*,[31] a 4-component Ugi reaction was used to prepare analogues bearing 4 different classes of covalent warheads (alkene Michael acceptor, α-halo ketone, alkyne Michael acceptor, and α-ketoamide, Scheme 1a).

Scheme 1[a]

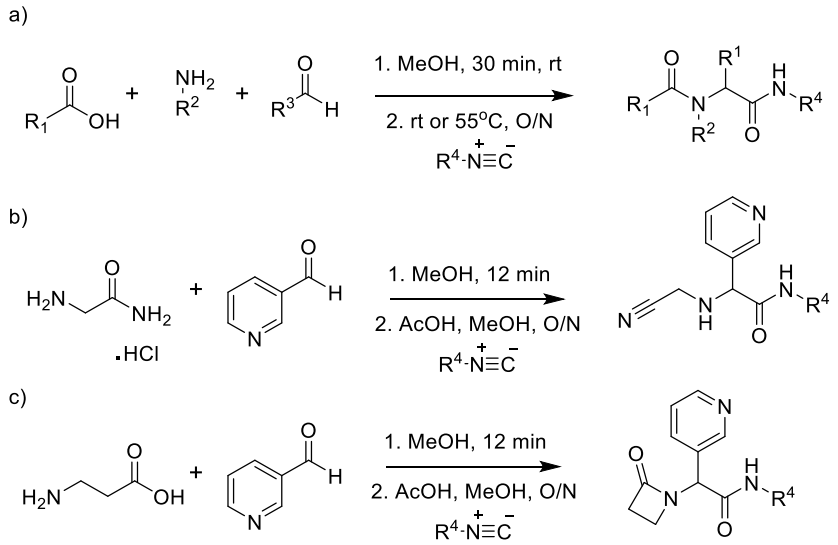

[a] a) carboxylic acid (1.0 mmol, 1.0 eq.), 4-*tert*-butylaniline (1.0 mmol, 1.0 eq.), 3-pyridinecarboxaldehyde (1.0 mmol, 1.0 eq.), cyclohexyl isocyanide (0.9 mmol, 0.9 eq.), MeOH (5 mL, 0.2 M), r.t., overnight. b) 3-pyridinecarboxaldehyde (2.0 mmol, 2.0 eq.), glycinamide hydrochloride (2.0 mmol, 2.0 eq.), triethylamine (2.0 mmol, 2.0 eq.), acetic acid (2.0 mmol, 2.0 eq.), cyclohexyl isocyanide (2.0 mmol, 2.0 eq.), MeOH (5 mL, 0.2 M), r.t., overnight, 79% yield. c) 3-pyridinecarboxaldehyde (1.0 mmol, 1.0 eq.), b-alanine (1.0 mmol, 1.0 eq.), cyclohexyl isocyanide (1.0 mmol, 1.0 eq.), MeOH (5 mL, 0.2 M), r.t., overnight, 54%.

A 3-component Ugi reaction was used to prepare the two additional analogues bearing a nitrile[34] and β-lactam[35] covalent warheads following reported procedures (Scheme 1b). This synthetic strategy was also employed to probe some of the features of this class of inhibitors. Thus the 3-pyrimidyl group was replaced by other heterocycles, the cyclohexyl was replaced by a *tert*-butyl group and the *tert*-butylphenyl was simplified into a toluyl.

Results and Discussions

3CL^{pro} inhibition. An initial screening of these various synthesized compounds at 50 μM resulted in several compounds bearing covalent warheads presenting greater than 50% inhibition of 3CL^{pro} activity (Tables 1 and Table 2). The most potent compounds (greater than 80% inhibition) were further evaluated and the fluorescence assay progress curves are shown in Figure S2).

Table 1. Inhibitory potency against SARS-CoV-2 3CL^{pro}. Evaluation of warheads.

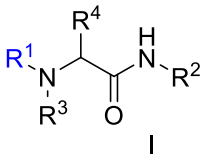

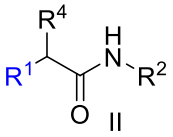

Entry	Scaffold	Cmpd	R^1	R^2	R^3	R^4	Inhibition (%)[a]	IC_{50} (μM)
1	I	**4**	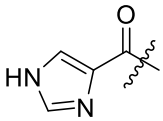	cHex	tBu-Ph	pyridin-3-yl	>95	4.1 ± 1.2
2	I	**5**	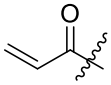	cHex	tBu-Ph	pyridin-3-yl	84 ± 1	11.1 ± 1.5
3	I	**6**	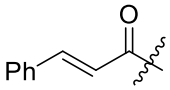	cHex	tBu-Ph	pyridin-3-yl	44 ± 6	nd[b]
4	I	**7**	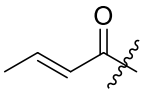	cHex	tBu-Ph	pyridin-3-yl	63 ± 5	nd[b]
5	I	**8**	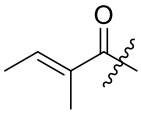	cHex	tBu-Ph	pyridin-3-yl	47 ± 2	nd[b]
6	I	**9**	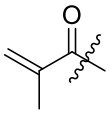	cHex	tBu-Ph	pyridin-3-yl	30 ± 1	nd[b]
7	I	**10**	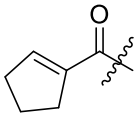	cHex	tBu-Ph	pyridin-3-yl	55 ± 10	nd[b]
8	I	**11**	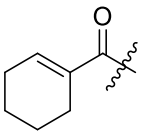	cHex	tBu-Ph	pyridin-3-yl	52 ± 1	nd[b]
9	I	**12**	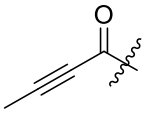	cHex	tBu-Ph	pyridin-3-yl	> 95%	5.3 ± 0.8

10	I	**13**	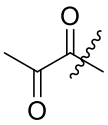	cHex	tBu-Ph	pyridin-3-yl	92 ± 1	5.2 ± 1.2
11	I	**14**	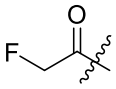	cHex	tBu-Ph	pyridin-3-yl	30 ± 7	nd[b]
12	I	**15**	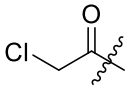	cHex	tBu-Ph	pyridin-3-yl	> 95	0.40 ± 0.16
13	I	**16**	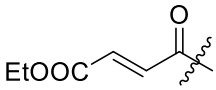	cHex	tBu-Ph	pyridin-3-yl	59 ± 6	nd[b]
14	I	**17**	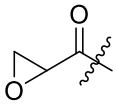	cHex	tBu-Ph	pyridin-3-yl		nd[b]
15	I	**18**		cHex	tBu-Ph	pyridin-3-yl	25 ± 8	nd[b]
16	II	**19**	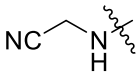	cHex	n/a	pyridin-3-yl	25 ± 1	nd[b]
17	II	**20**	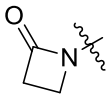	cHex	n/a	pyridin-3-yl	< 5	nd[b]

[a] The enzyme activity was measured with 150nM 3CL^{pro} and 50 μM of each potential inhibitor. [b] not determined.

Table 2. Inhibitory potency against SARS-CoV-2 3CL^{pro}. Optimization of side chains.

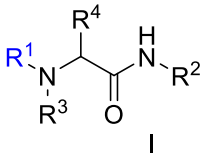

I

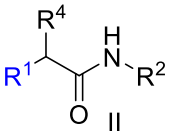

II

Entry	Scaffold	Cmpd	R^1	R^2	R^3	R^4	Inhibition (%)[a]	IC_{50} (μM)
1	I	**21**	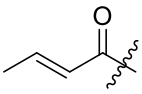	tBu	tBu-Ph	pyridin-3-yl	33 ± 1	nd[b]
2	I	**22**	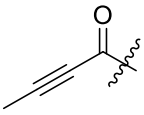	tBu	tBu-Ph	pyridin-3-yl	93	15.0 ± 9.3

3	I	**23**	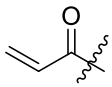	tBu	tBu-Ph	pyridin-3-yl	68 ± 1	nd[b]
4	I	**24**	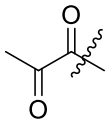	cHex	tBu-Ph	tolu-3-yl	< 5%	nd[b]
5	I	**25**	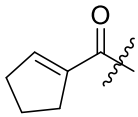	cHex	tBu-Ph	thiophen-3-yl	22 ± 8	nd[b]
6	I	**26**	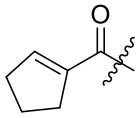	cHex	tBu-Ph	quinolin-3-yl	18 ± 8	nd[b]
7	I	**27**	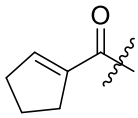	cHex	tBu-Ph	benzo[d]thiazol-2-yl	< 5	nd[b]
8	I	**28**	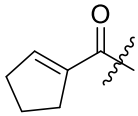	cHex	tBu-Ph	pyridin-4-yl	19 ± 8	nd[b]
9	I	**29**	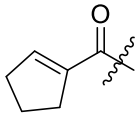	cHex	tBu-Ph	pyrimidin-5-yl	38 ± 8	nd[b]
10	I	**30**	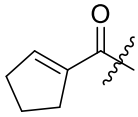	cHex	tBu-Ph	isoquinolin-4-yl	< 5	nd[b]
11	I	**31 (ML188)**	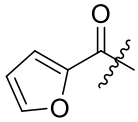	tBu	tBu-Ph	pyridin-3-yl	> 95	1.4 ± 0.4
12	I	**32**	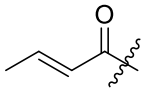	tBu	tBu-Ph	pyridin-4-yl	24 ± 8	nd[b]
13	I	**33**		tBu	tBu-Ph	pyridin-3-yl	< 5	nd[b]
14	I	**34**	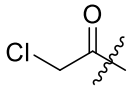	cHex	tBu-Ph	thiophen-3-yl	22 ± 11	nd[b]
15	I	**35**	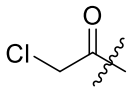	cHex	tBu-Ph	pyridin-4-yl	91 ± 1	0.91 ± 0.12

16	I	**36**	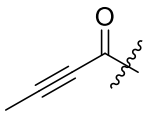	cPent	tBu-Ph	pyridin-3-yl	> 95	1.17 ± 0.26
17	I	**37**	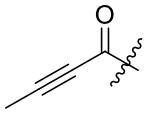	Bn	tBu-Ph	pyridin-3-yl	93± 1	9.5 ± 0.9
18	I	**38**	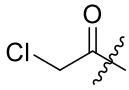	cPent	tBu-Ph	pyridin-3-yl	> 95	1.07 ± 0.65
19	I	**39**	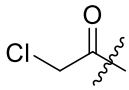	Bn	tBu-Ph	pyridin-3-yl	> 95	0.38 ± 0.09
20	I	**40**	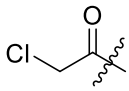	cHex	tBu-Ph	5-methylpyrazin-2-yl	80 ± 4	15 ± 5

[a] The enzyme activity was measured with 150nM 3CL^{pro} and 50 μM of each potential inhibitor. [b] not determined.

IC_{50} values (evaluated at 11.7 μM substrate concentration) for the most promising inhibitors were evaluated and results are reported in Table 1. First, we observed that **3** and **31**, previously reported as low micromolar SARS-CoV 3CL^{pro} inhibitors (IC_{50} = 3.4 μM[36] and IC_{50} = 4.8 μM[31] respectively), also inhibit SARS-CoV-2 3CL^{pro} with similar potencies. Gratifyingly, some of the designed inhibitors, in particular **5**, **12, 13, 15**, **22** and **35**, also inhibited SARS-CoV-2 3CL^{pro}, some even with potency higher than the original non-covalent inhibitor. The most reactive and least hindered warheads (acrylamide, alkynylamide, α-chloro ketone and ketoamide) showed the highest activity, Inhibitor **15** was the most potent (**15**: IC_{50} = 0.4 μM), an order of magnitude over the original non-covalent hit molecule (**4**: IC_{50} = 4.1 μM).

Another observation is the significant loss of potency when removing the imidazole ring (compounds **4** vs. **33**). This observation is consistent with our analysis of the role of this heterocycle mentioned above (Figure 2). Substitution of this heterocycle with a carbocycle of similar size but no hydrogen bonding groups (compounds **10** vs. **4**) does not preserve the inhibitory potency even when this ring was converted to a warhead for covalent binding.

We also observed that the activity of compounds with Michael acceptor warheads (eg, **5** and **12**) was not improved over the non-covalent inhibitor. This is not unexpected as the catalytic cysteine is near the

carbon of the imidazole adjacent to the carbonyl in **4** (crystal structure, Figure 2), while a conjugate addition requires making a bond with the more distant carbon atom which would not interact with the oxy-anion hole as does the imidazole ring. Unfortunately, the ketoamide **13**, a warhead which fulfills these geometrical restrictions, does not exhibit a significant increase in potency, although the Michael acceptors would act as irreversible inhibitors while the ketoamide is more likely a reversible inhibitor. We further selected a Michael acceptor warhead (**16**) which would properly position the reactive carbon next to the catalytic cysteine including an epoxide (**17**). Unfortunately, this strategy did not improve the potency and the irreversible α-chloro amide derivative remains the most potent.

In parallel to the search for an optimal warhead, several modifications were made to the core of the molecule (Table 2). Previously, it was shown that replacement of the *t*BuPh group (R^3 in Table 1) by smaller groups or differently substituted phenyl groups modulates the potency against SARS-CoV 3CL^{pro} with slight improvements in some cases, while various hydrophobic groups were tolerated as R^2.[36] We thought this information could help further improve these inhibitors for the highly homologous SARS-CoV-2 3CL^{pro}. However, any attempt to improve the side groups has proven unsuccessful to date; a single modification (**39**) led to a compound equipotent to **15**.

Covalent binding. In order to evaluate the covalent inhibition hypothesis, we measured the time dependence of the inhibition of our most potent inhibitor, **15**. As can be seen in Figure 6, the level of inhibition increases over time when the inhibitor is used close to its IC_{50} concentration, while it remains constant for the non-covalent inhibitor **4**. This observation is consistent with the slow formation of a covalent adduct. Furthermore, mass spectrometry (MS) experiments were conducted to detect the presence of the 3CL^{pro}-**15** adduct (Figure S3). When the protease was incubated with inhibitor **15**, the population of intact protein decreases as a new population with higher mass (3CL^{pro} + **15** – HCl) appears which was maintained after a denaturation treatment (Figure S3).

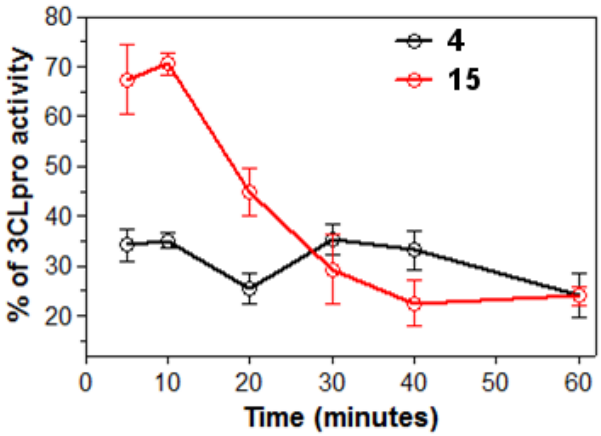

Figure 6. Time-dependent potency for **4** and **15**.

Isothermal Titration Calorimetry (ITC). ITC was employed to validate the initial fluorescence inhibition assay. ITC provides unique insights into the kinetics and thermodynamics of inhibitor binding that are not available in traditional enzyme assays.[37] ITC experiments measure the heat flow or power produced by catalysis as a function of time (Figure 7, y- and *x*-axis, respectively), as one component is titrated into another. The power is proportional to the enzyme velocity, with larger deflections corresponding to higher velocities. Exothermic and endothermic reactions giving downward and upward deflections of the ITC signal, respectively. Since the instrument detects the heat released by the native reaction, unlabeled substrates can be used in the experiments, unlike the fluorescence assay which requires substrates modified with large hydrophobic dyes and quenchers.

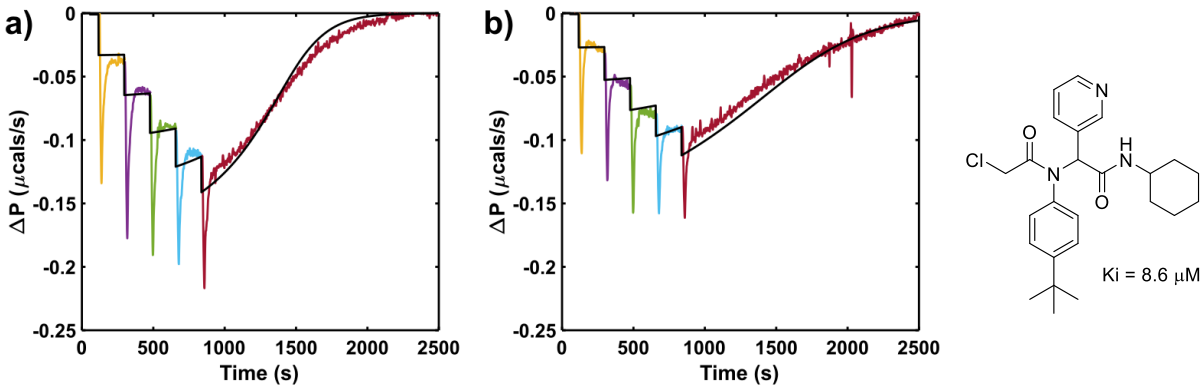

Figure 7. ITC enzyme activity assay in the presence of a) no inhibitor, b) 10 uM **15**, each successive injection is shown in separate color, while kinetic ITC simulations according to the minimized Michaelis-Menten parameters are shown as black curves.

We performed activity assays where enzyme was added in a series of injections to the sample cell, which contained either substrate alone or a mixture of substrate and 15. In these experiments, the

reaction rate increased with each injection due to the increase in enzyme concentration (data following each injection have a different color in Figure 7). The reaction rate decreased after the final injection and returned to the initial baseline as all of the substrate was consumed. We fitted the resulting traces to extract Michaelis Menten kinetic parameters (black curves), as described in the Methods Section. The apparent value of Km was roughly twice as large in the presence **15**, due to competitive inhibition, and corresponds to a Ki of 8.6 μM. This Ki is more than an order of magnitude greater than the one obtained from the fluorescent assay. This is consistent with our observation that the level of inhibition is initially modest (≈ 30%) and increases over the course of roughly 30 minutes to reach ≈ 75% (Figure 6). The fluorescence-based IC50 values were obtained with a 30 minute pre-incubation of enzyme and inhibitor. In contrast, ITC reports the initial or instantaneous level of inhibition when enzyme and 15 are first mixed. Interestingly, the ITC-based value is on the order of the IC_{50} value of the non-covalent parent compound (4) Together, these data are consistent with a model in which 15 first binds 3CLpro non-covalently with low micromolar affinity, followed by a slow formation of the covalent bond, giving an apparent IC_{50} of 0.4 μM after 30 minutes.

Conclusion

Covalent inhibition of SARS-CoV-2 3CL^{pro} is a promising strategy for the treatment of COVID-19. Our strategy relied on a previously reported imidazole-containing inhibitor of the similar coronavirus SARS-CoV responsible for the epidemic of SARS in the early 2000's. We first used our docking program FITTED, specifically modified to accommodate covalent inhibitors, and screened a set of covalent warheads. The docked poses confirmed that replacing the imidazole ring by a reactive group should lead to potent covalent inhibition. Gratifyingly, while the imidazole was known to be essential for the inhibitory potency, replacing it with many warheads maintained and even improved the potency, with our lead compound **15** being an order of magnitude more potent. Both, the inhibition pattern of enzymatic activity and the biophysical data suggests that this inhibitor binds covalently to the viral protease; thus, the robustness of *in silico* rational-drug design was validated using *in vitro* detection of protein processing.

Experimental section

Synthesis and characterization

General Considerations. All other reagents were purchased from commercial suppliers and used without further purification. All ^{1}H and ^{13}C NMR spectra were acquired Bruker Avance 500 MHz spectrometer. Chemical shifts are reported in ppm using the residual of deuterated solvents as an internal standard. Chromatography was performed on silica gel 60 (230-40 mesh) or using the Biotage One Isolera with ZIP cartridges. High resolution mass spectrometry was performed by ESI on a Bruker Maxis Impact API QqTOF or by ESI or APCI on a ThermoFisher Exactive Plus Orbitrap-API at McGill University

General Procedure for 4-Component Ugi Reaction. In a 6-dram vial equipped with a stir bar aldehyde (1.0 mmol, 1.0 eq.), aniline (1.0 mmol, 1.0 eq.) and carboxylic acid (1.0 mmol, 1.0 eq.) were combined in MeOH (4 mL). The obtained reaction mixture was stirred for 30 min at room temperature. Afterwards cyclohexyl isocyanide (0.9 mmol, 0.9 eq.) was added to the reaction mixture and the walls of the vial were washed with 1 mL of MeOH. The reaction mixture was continued to stir at room temperature overnight. The crude reaction mixture was evaporated in vacuo. Purification procedure A) The crude product was triturated with hexanes (5 mL) and filtered. The obtained product was further washed with hexanes (3 x 3 mL). Purification procedure B) The crude product recrystallized from $CHCl_3$/Hexanes mixture, filtered and the obtained product was further washed with hexanes (3 x 3 mL). Purification procedure C) The crude product was redissolved in DCM. The obtained crude solution was deposited on silica. It was then purified using flash column chromatography using DCM/MeOH (gradient 0 → 5%) as eluent.

***N*-(4-(*tert*-butyl)phenyl)-*N*-(2-(cyclohexylamino)-2-oxo-1-(pyridin-3-yl)ethyl)-1H-imidazole-5-carboxamide (4).** ^{1}H NMR (500 MHz, MeOD) δ 8.37 (s, 1H), 8.33 (dd, *J* = 4.9, 1.5 Hz, 1H), 7.66 – 7.57 (m, 2H), 7.31 (d, *J* = 7.8 Hz, 2H), 7.22 (dd, J = 7.9, 4.9 Hz, 1H), 6.27 (s, 1H), 5.46 (s, 1H), 3.71 (td, *J* = 10.5, 9.3, 3.9 Hz, 1H), 1.93 (d, *J* = 12.3 Hz, 1H), 1.80 – 1.72 (m, 2H), 1.65 (ddt, *J* = 30.9, 12.9, 3.8 Hz, 2H), 1.27 (s, 12H). ^{13}C NMR (126 MHz, MeOD) δ 169.00, 152.54, 150.62, 148.24, 138.83, 136.36, 131.58, 131.07, 125.72, 123.31, 62.74, 34.16, 32.16, 32.12, 30.25, 25.22, 24.72, 24.64. HRMS (ESI+) for $C_{27}H_{33}N_5NaO_2$ (M + Na) calculated 482.2526; found 482.2535.

***N*-(4-(*tert*-butyl)phenyl)-*N*-(2-(cyclohexylamino)-2-oxo-1-(pyridin-3-yl)ethyl) acrylamide (5).** Compound was purified using general procedure C, white solid 32 % yield, 120 mg. ^{1}H NMR (500 MHz, $CDCl_3$) δ 8.41 – 8.39 (m, 1H), 8.38 – 8.37 (m, 1H), 7.42 – 7.35 (m, 1H), 7.19 (d, *J* = 8.1 Hz, 2H), 7.01 (dd, *J* = 8.0, 4.8 Hz, 1H), 6.91 (s, 1H), 6.49 (d, *J* = 8.0 Hz, 1H), 6.33 (dd, *J* = 16.8, 2.0 Hz, 1H),

6.11 (s, 1H), 5.93 (dd, *J* = 16.8, 10.3 Hz, 1H), 5.49 (dd, *J* = 10.4, 2.0 Hz, 1H), 3.84 – 3.73 (m, 1H), 1.93 (s, 1H), 1.81 (dd, *J* = 13.1, 4.1 Hz, 1H), 1.67 – 1.53 (m, 3H), 1.37 – 1.26 (m, 2H), 1.22 (s, 9H), 1.17 – 1.06 (m, 3H). ^{13}C NMR (126 MHz, $CDCl_3$) δ 168.04, 166.50, 151.79, 151.28, 149.45, 137.93, 136.14, 130.83, 129.93, 128.64, 128.52, 126.08, 122.85, 62.69, 48.76, 34.64, 32.86, 32.80, 31.27, 25.52, 24.83, 24.77. HRMS (ESI+) for $C_{26}H_{33}N_3NaO_2$ (M + Na) calculated 442.2465; found 442.2456.

***N*-(4-(*tert*-butyl)phenyl)-*N*-(2-(cyclohexylamino)-2-oxo-1-(pyridin-3-yl)ethyl) cinnamamide (6).** Compound was purified using general procedure A, pale white solid 94 % yield, 420 mg. ^{1}H NMR (500 MHz, $CDCl_3$) δ 8.48 (d, *J* = 2.3 Hz, 1H), 8.47 (dd, *J* = 4.8, 1.7 Hz, 1H), 7.71 (d, *J* = 15.6 Hz, 1H), 7.50 (dt, *J* = 7.9, 2.0 Hz, 1H), 7.27 (s, 6H), 7.07 (dd, *J* = 8.0, 4.8 Hz, 1H), 6.98 (s, 1H), 6.33 (d, *J* = 8.1 Hz, 1H), 6.24 (d, *J* = 15.5 Hz, 1H), 6.14 (s, 1H), 3.91 – 3.80 (m, 1H), 1.94 (dd, *J* = 52.0, 13.0 Hz, 2H), 1.70 (ddd, *J* = 18.3, 11.4, 6.7 Hz, 2H), 1.59 (dd, *J* = 8.9, 4.1 Hz, 1H), 1.44 – 1.32 (m, 2H), 1.29 (s, 9H), 1.26 – 1.09 (m, 4H). ^{13}C NMR (126 MHz, CDCl3) δ 168.16, 167.14, 151.97, 151.36, 149.60, 143.22, 138.03, 136.60, 135.07, 130.93, 129.91, 129.86, 128.82, 128.13, 126.35, 122.95, 118.61, 63.32, 48.85, 34.81, 33.02, 32.96, 31.38, 25.62, 24.90, 24.86. HRMS (ESI+) for $C_{32}H_{37}N_3NaO_2$ (M + Na) calculated 518.2778; found 518.2790.

(*E*)-*N*-(4-(*tert*-butyl)phenyl)-*N*-(2-(cyclohexylamino)-2-oxo-1-(pyridin-3-yl)ethyl)but-2-enamide (7). Compound was purified using general procedure B, pale white solid 32 % yield, 126 mg. ^{1}H NMR (500 MHz, CDCl3) δ 8.46 – 8.41 (m, 2H), 7.44 (dt, J = 7.9, 2.0 Hz, 1H), 7.24 (d, J = 8.2 Hz, 2H), 7.04 (ddd, J = 8.0, 4.8, 0.8 Hz, 1H), 6.99 – 6.91 (m, 3H), 6.36 (d, J = 8.1 Hz, 1H), 6.09 (s, 1H), 5.65 (dd, J = 15.0, 1.7 Hz, 1H), 3.87 – 3.76 (m, 1H), 1.97 (dd, J = 11.7, 4.6 Hz, 1H), 1.92 – 1.82 (m, 1H), 1.72 (dd, J = 7.0, 1.7 Hz, 3H), 1.69 – 1.63 (m, 1H), 1.60 – 1.56 (m, 1H), 1.42 – 1.30 (m, 2H), 1.27 (s, 9H), 1.22 – 1.09 (m, 3H). ^{13}C NMR (126 MHz, $CDCl_3$) δ 168.25, 166.99, 151.78, 151.24, 149.41, 143.08, 138.09, 136.62, 131.00, 129.80, 126.22, 122.88, 122.71, 62.96, 48.78, 34.75, 32.97, 32.91, 31.37, 25.62, 24.88, 24.84, 18.21. HRMS (ESI+) for $C_{27}H_{35}N_3NaO_2$ (M + Na) calculated 456.2621; found 456.2630.

(*E*)-*N*-(4-(*tert*-butyl)phenyl)-*N*-(2-(cyclohexylamino)-2-oxo-1-(pyridin-3-yl)ethyl)-2-methylbut-2-enamide (8). Compound was purified using general procedure A, white solid 73 % yield, 294 mg. ^{1}H NMR (500 MHz, $CDCl_3$) δ 8.50 (d, *J* = 2.3 Hz, 1H), 8.49 – 8.45 (m, 1H), 7.55 (dt, *J* = 7.9, 2.0 Hz, 1H), 7.17 (d, *J* = 8.8 Hz, 2H), 7.10 (ddd, *J* = 7.9, 4.8, 0.8 Hz, 1H), 6.87 (d, *J* = 8.1 Hz, 2H), 6.29 (d, *J* = 8.2 Hz, 1H), 5.98 (s, 1H), 5.77 (dddd, *J* = 8.5, 6.9, 5.5, 1.6 Hz, 1H), 3.90 – 3.79 (m, 1H), 1.96 (d, *J* = 9.1 Hz, 1H), 1.92 – 1.87 (m, 1H), 1.74 – 1.55 (m, 3H), 1.51 (s, 3H), 1.45 (dd, *J* = 6.9, 1.2 Hz, 3H), 1.44 – 1.30

(m, 2H), 1.24 (s, 9H), 1.23 – 1.08 (m, 3H). ^{13}C NMR (126 MHz, $CDCl_3$) δ 174.17, 168.17, 151.06, 150.92, 149.49, 138.40, 137.72, 132.44, 131.30, 131.17, 128.98, 125.80, 123.03, 64.28, 34.67, 33.00, 32.98, 31.36, 25.63, 24.86, 24.81, 14.17, 13.46. HRMS (ESI+) for $C_{28}H_{37}N_3NaO_2$ (M + Na) calculated 470.2778; found 470.2766.

***N*-(4-(*tert*-butyl)phenyl)-*N*-(2-(cyclohexylamino)-2-oxo-1-(pyridin-3-yl)ethyl) methacrylamide (9)**. Compound was purified using general procedure B, pale white solid 68 % yield, 265 mg. ^{1}H NMR (500 MHz, MeOD) δ 8.33 (d, *J* = 2.3 Hz, 1H), 8.31 (dd, *J* = 4.9, 1.6 Hz, 1H), 7.56 (dt, *J* = 7.9, 2.0 Hz, 1H), 7.23 – 7.15 (m, 3H), 7.05 (s, 2H), 6.10 (s, 1H), 5.01 (dt, *J* = 6.9, 1.3 Hz, 2H), 3.70 (tt, *J* = 10.9, 3.9 Hz, 1H), 1.90 (dd, *J* = 10.7, 3.8 Hz, 1H), 1.73 (s, 5H), 1.70 – 1.59 (m, 2H), 1.41 – 1.27 (m, 3H), 1.21 (s, 9H), 1.19 – 1.06 (m, 2H). ^{13}C NMR (126 MHz, $CDCl_3$) δ 172.82, 167.95, 151.29, 151.19, 149.55, 140.42, 137.86, 137.64, 130.88, 129.32, 125.77, 122.97, 119.77, 63.47, 48.78, 34.63, 32.90 (d, *J* = 10.4 Hz),, 31.32, 25.57, 24.83, 24.77, 20.42. HRMS (ESI+) for $C_{27}H_{35}N_3NaO_2$ (M + Na) calculated 456.2621; found 456.2620.

***N*-(4-(tert-butyl)phenyl)-*N*-(2-(cyclohexylamino)-2-oxo-1-(pyridin-3-yl)ethyl)cyclopent-1-ene-1-carboxamide (10).** Compound was purified using general procedure A, pale yellow solid 80 % yield, 333 mg. ^{1}H NMR (500 MHz, CDCl3) δ 8.48 (d, J = 2.3 Hz, 1H), 8.46 (dd, J = 4.8, 1.7 Hz, 1H), 7.51 (dt, J = 8.0, 2.0 Hz, 1H), 7.21 – 7.16 (m, 2H), 7.08 (ddd, J = 7.9, 4.8, 0.8 Hz, 1H), 6.90 (d, J = 8.0 Hz, 2H), 6.28 (d, J = 8.0 Hz, 1H), 6.04 (s, 1H), 5.82 (d, J = 2.3 Hz, 1H), 3.89 – 3.78 (m, 1H), 2.19 (ddt, J = 7.7, 5.1, 2.5 Hz, 2H), 2.12 (tt, J = 6.7, 2.8 Hz, 2H), 2.02 – 1.93 (m, 1H), 1.92 – 1.84 (m, 1H), 1.73 – 1.54 (m, 4H), 1.44 – 1.29 (m, 2H), 1.25 (s, 9H), 1.23 – 1.07 (m, 3H). ^{13}C NMR (126 MHz, CDCl3) δ 168.92, 168.16, 151.57, 151.22, 149.46, 140.13, 139.09, 137.96, 137.69, 130.98, 129.50, 125.81, 122.94, 63.92, 48.74, 34.69, 33.80, 33.22, 32.95, 32.92, 31.35, 25.60, 24.84, 24.79, 23.29. HRMS (ESI+) for $C_{29}H_{37}N_3NaO_2$ (M + Na) calculated 482.2778; found 482.2781.

***N*-(4-(*tert*-butyl)phenyl)-*N*-(2-(cyclohexylamino)-2-oxo-1-(pyridin-3-yl)ethyl)cyclohex-1-ene-1-carboxamide (11).** Compound was purified using general procedure A, white solid 37 % yield, 157 mg. ^{1}H NMR (500 MHz, $CDCl_3$) δ 8.50 (d, *J* = 2.3 Hz, 1H), 8.47 (dd, *J* = 4.8, 1.6 Hz, 1H), 7.55 (dt, *J* = 8.0, 2.0 Hz, 1H), 7.18 (d, *J* = 8.8 Hz, 2H), 7.11 (ddd, *J* = 7.9, 4.8, 0.8 Hz, 1H), 6.88 (d, *J* = 8.1 Hz, 2H), 6.30 (d, *J* = 8.2 Hz, 1H), 6.00 (s, 1H), 5.84 (dt, *J* = 3.8, 2.0 Hz, 1H), 3.90 – 3.79 (m, 1H), 1.99 – 1.80 (m, 5H), 1.75 – 1.54 (m, 6H), 1.44 – 1.29 (m, 4H), 1.25 (s, 9H), 1.24 – 1.13 (m, 3H). ^{13}C NMR (126 MHz, $CDCl_3$) δ 173.52, 168.18, 151.11, 151.05, 149.50, 138.33, 137.79, 134.48, 133.17, 131.12, 129.08,

125.69, 123.02, 63.95, 48.72, 34.68, 33.01, 32.97, 31.37, 26.14, 25.64, 25.00, 24.85, 22.04, 21.45. HRMS (ESI+) for $C_{30}H_{39}N_3NaO_2$ (M + Na) calculated 496.2934; found 496.2931.

***N*-(4-(*tert*-butyl)phenyl)-*N*-(2-(cyclohexylamino)-2-oxo-1-(pyridin-3-yl)ethyl)but-2-ynamide (12).** Compound was purified using general procedure A, white solid 92 % yield, 357 mg. ^{1}H NMR (500 MHz, $CDCl_3$) δ 8.44 (d, *J* = 4.9 Hz, 1H), 8.41 (d, *J* = 2.3 Hz, 1H), 7.44 (d, *J* = 8.1 Hz, 1H), 7.21 (d, *J* = 8.4 Hz, 2H), 7.05 (dd, *J* = 8.0, 4.8 Hz, 1H), 6.97 (d, *J* = 8.0 Hz, 2H), 6.20 (s, 1H), 6.03 (s, 1H), 3.80 (dtd, *J* = 10.8, 7.2, 4.0 Hz, 1H), 1.96 (dq, *J* = 13.2, 4.8 Hz, 1H), 1.84 (d, *J* = 16.6 Hz, 1H), 1.75 – 1.62 (m, 5H), 1.58 (dd, *J* = 13.1, 4.1 Hz, 1H), 1.42 – 1.26 (m, 2H), 1.25 (s, 9H), 1.25 – 1.05 (m, 3H). ^{13}C NMR (126 MHz, $CDCl_3$) δ 167.43, 155.41, 151.87, 151.20, 149.62, 138.15, 136.38, 130.34, 129.90, 125.70, 122.98, 92.12, 73.86, 62.23, 34.71, 32.87, 32.80, 31.31, 25.56, 24.85, 24.80. HRMS (ESI+) for $C_{27}H_{33}N_3NaO_2$ (M + Na) calculated 454.2465; found 454.2458.

***N*-(4-(*tert*-butyl)phenyl)-*N*-(2-(cyclohexylamino)-2-oxo-1-(pyridin-3-yl)ethyl)-2-oxopropanamide (13).** To a solution of 4-tert-butylaniline (0.10 mL, 0.67 mmol, 1.0 eq.) in MeOH (2 mL) was added 3-pyridine carboxaldehyde (0.06 mL, 0.67 mmol, 1.0 eq.) and the solution stirred at room temperature for 30 minutes. The solution was cooled to 0 ºC, and pyruvic acid (0.06 mL, 0.80 mmol, 1.2 eq.) and cyclohexyl isocyanide (0.10 mL, 0.80 mmol, 1.2 eq.) were added in quick succession. The solution was slowly warmed to room temperature and stirred overnight. The crude reaction mixture was evaporated in vacuo and purified by column chromatography (1:1 Hex:EtOAc) to afford the product (105 mg, 36%) as a white powder. ^{1}H NMR (500 MHz, $CDCl_3$) δ 8.69 (s, 1H), 8.56 (s, 1H), 7.84 (d, *J* = 8.0 Hz, 1H), 7.35 (d, *J* = 7.7 Hz, 1H), 7.23 (d, *J* = 8.8 Hz, 2H), 7.03 (d, *J* = 8.1 Hz, 2H), 6.49 (d, *J* = 8.0 Hz, 1H), 6.15 (s, 1H), 3.80 (tdd, *J* = 10.7, 6.7, 4.0 Hz, 1H), 2.19 (s, 3H), 1.97 – 1.79 (m, 2H), 1.69 (ddt, *J* = 17.1, 13.1, 4.0 Hz, 2H), 1.59 (dt, *J* = 12.8, 3.9 Hz, 1H), 1.41 – 1.25 (m, 2H), 1.24 (s, 9H), 1.16 (dtd, *J* = 16.2, 13.6, 12.7, 9.9 Hz, 2H).^{13}C NMR (126 MHz, $CDCl_3$) δ 197.49, 168.14, 166.68, 152.69, 150.19, 148.63, 139.25, 134.15, 130.64, 129.82, 126.29, 123.61, 62.36, 49.22, 34.77, 32.85, 32.81, 31.26, 27.84, 25.51, 24.87, 24.81. HRMS (ESI+) for $C_{26}H_{33}N_3NaO_3$ (M + Na) calculated 458.2412; found 458.2421

***N*-(4-(tert-butyl)phenyl)-*N*-(2-(cyclohexylamino)-2-oxo-1-(pyridin-3-yl)ethyl)-2-fluoroacetamide (14).** Compound was purified using general procedure A, pale yellow solid 70 % yield, 270 mg. ^{1}H NMR (500 MHz, $CDCl_3$) δ 8.47 (dd, *J* = 4.9, 1.7 Hz, 1H), 8.43 (d, *J* = 2.3 Hz, 1H), 7.43 (dt, *J* = 7.9, 2.0 Hz, 1H), 7.24 (s, 2H), 7.06 (ddd, *J* = 8.0, 4.8, 0.8 Hz, 1H), 6.04 (s, 1H), 5.87 (d, *J* = 7.8 Hz, 1H), 4.64 (d,

J = 3.1 Hz, 1H), 4.55 (d, *J* = 3.3 Hz, 1H), 3.86 – 3.75 (m, 1H), 2.02 – 1.95 (m, 1H), 1.89 – 1.81 (m, 1H), 1.74 – 1.55 (m, 3H), 1.44 – 1.28 (m, 2H), 1.25 (s, 9H), 1.22 – 1.02 (m, 3H). ^{13}C NMR (126 MHz, $CDCl_3$) δ 168.05, 167.89, 167.48, 153.00, 151.45, 149.99, 138.13, 133.76, 129.97, 129.82, 126.64, 123.12, 78.70 (d, *J* = 178.1 Hz), 62.38, 49.16, 34.84, 32.94 (d, *J* = 9.3 Hz), 31.31, 25.57, 24.90 (d, *J* = 6.9 Hz).HRMS (ESI+) for $C_{25}H_{32}FN_3NaO_2$ (M + Na) calculated 448.2371; found 448.2366.

***N*-(4-(*tert*-butyl)phenyl)-2-chloro-*N*-(2-(cyclohexylamino)-2-oxo-1-(pyridin-3-yl)ethyl) acetamide (15).** Compound was purified using general procedure A, yellow solid 93 % yield, 370 mg. ^{1}H NMR (500 MHz, $CDCl_3$) δ 8.47 (dd, *J* = 4.8, 1.6 Hz, 1H), 8.43 (d, *J* = 2.3 Hz, 1H), 7.44 (dt, *J* = 7.9, 2.0 Hz, 1H), 7.26 (s, 3H), 7.07 (ddd, *J* = 7.8, 4.9, 0.8 Hz, 1H), 5.99 (s, 1H), 5.88 (s, 1H), 3.85 (s, 2H), 3.84 – 3.78 (m, 1H), 1.98 (dd, *J* = 12.6, 4.2 Hz, 1H), 1.85 (dd, *J* = 12.6, 4.2 Hz, 1H), 1.74 – 1.63 (m, 2H), 1.59 (dt, *J* = 12.8, 3.8 Hz, 1H), 1.43 – 1.28 (m, 2H), 1.26 (s, 9H), 1.22 – 1.03 (m, 3H). ^{13}C NMR (126 MHz, CDCl3) δ 167.43, 167.42, 152.83, 151.27, 149.75, 138.27, 135.35, 130.28, 129.73, 126.61, 123.16, 63.16, 49.11, 42.58, 34.84, 32.97, 32.90, 31.33, 25.57, 24.91, 24.85. HRMS (ESI+) for $C_{25}H_{32}ClN_3NaO_2$ (M + Na) calculated 464.2075; found 464.2087.

Ethyl (*E*)-4-((4-(*tert*-butyl)phenyl)(2-(cyclohexylamino)-2-oxo-1-(pyridin-3-yl)ethyl)amino)-4-oxobut-2-enoate (16). Product purified using general procedure A, white powder 52% yield, 170 mg. ^{1}H NMR (500 MHz, $CDCl_3$) δ 8.51 – 8.38 (m, 2H), 7.49 (dt, *J* = 8.1, 2.0 Hz, 1H), 7.23 (d, *J* = 8.1 Hz, 2H), 7.09 (dd, *J* = 8.0, 4.8 Hz, 1H), 6.85 (d, *J* = 15.3 Hz, 1H), 6.72 (d, *J* = 15.3 Hz, 1H), 6.24 (d, *J* = 8.1 Hz, 1H), 6.10 (s, 1H), 4.12 (q, *J* = 7.1 Hz, 2H), 3.80 (dtd, *J* = 10.8, 7.2, 4.0 Hz, 1H), 1.98 – 1.90 (m, 1H), 1.89 – 1.79 (m, 1H), 1.72 – 1.53 (m, 3H), 1.33 (ddd, *J* = 13.0, 10.0, 3.3 Hz, 1H), 1.25 (s, 9H), 1.20 (t, *J* = 7.1 Hz, 3H), 1.10 (ddt, *J* = 23.0, 15.4, 10.8 Hz, 1H). ^{13}C NMR (126 MHz, $CDCl_3$) δ 167.37, 165.46, 165.04, 152.42, 150.54, 148.89, 138.83, 135.41, 133.89, 132.15, 130.95, 129.77, 126.48, 123.26, 63.08, 61.13, 49.00, 34.77, 32.90, 32.84, 31.28, 25.53, 24.86, 24.80, 14.11.HRMS (ESI+): $C_{29}H_{37}N_3NaO_4$ $(M+Na)^+$ calculated 514.2676; found 514.2691.

2-(*N*-(4-(*tert*-butyl)phenyl)acetamido)-*N*-cyclohexyl-2-(pyridin-3-yl)acetamide (18). Compound was purified using general procedure A, white solid 76 % yield, 280 mg. ^{1}H NMR (500 MHz, $CDCl_3$) δ 8.46 – 8.43 (m, 1H), 8.42 (s, 1H), 7.41 (d, *J* = 8.1 Hz, 1H), 7.23 (d, *J* = 8.5 Hz, 2H), 7.03 (dd, *J* = 8.0, 4.8 Hz, 1H), 6.93 (s, 1H), 6.03 (s, 2H), 3.94 – 3.65 (m, 1H), 1.98 (d, *J* = 16.8 Hz, 1H), 1.89 – 1.81 (m, 4H), 1.75 – 1.63 (m, 2H), 1.59 (dt, *J* = 13.0, 4.3 Hz, 1H), 1.43 – 1.28 (m, 2H), 1.25 (s, 9H), 1.23 – 1.04 (m, 3H). ^{13}C NMR (126 MHz, $CDCl_3$) δ 171.83, 168.21, 151.89, 151.44, 149.66, 138.09, 137.42,

130.87, 129.60, 126.28, 122.92, 62.42, 48.88, 34.73, 32.95 (d, *J* = 10.4 Hz), 31.37, 25.61, 24.87 (d, *J* = 6.9 Hz), 23.34. HRMS (ESI+) for $C_{25}H_{33}N_3NaO_2$ (M + Na) calculated 430.2465; found 430.2464.

***N*-cyclohexyl-2-(2-oxoazetidin-1-yl)-2-(pyridin-3-yl)acetamide (18).** In a 6-dram vial equipped with a stir bar 3-Pyridinecarboxaldehyde (214 mg, 2.0 mmol, 1.0 eq.), glycinamide hydrochloride (221 mg, 2.0 mmol, 1.0 eq.), and triethylamine (202 mg, 2.0 mmol, 1.0 eq.), were mixed together in methanol (5 mL). The obtained solution was stirred for 15 min at room temperature. Afterwards cyclohexyl isocyanide (218 mg, 2.0 mmol, 1.0 eq.), and acetic acid (120 mg, 2.0 mmol, 1.0 eq.) was added to the reaction mixture and the walls of the vial were washed with additional MeOH (5 mL). The reaction mixture was stirred at room temperature overnight. The crude reaction mixture was evaporated in vacuo and redissolved in EtOAc (50 mL). The organic layer was extracted with water (3 x 100 mL). The obtained organic layer was dried over Na_2SO_4 and evaporated in vacuo. The obtained crude solid was triturated with hexanes (5 mL) and filtered. The Obtained powder was further washed Hexanes (2 x 5 mL). The product was obtained as pale-yellow solid, 428 mg 79%. ^{1}H NMR (500 MHz, $CDCl_3$) δ 8.59 (s, 2H), 7.75 (dd, *J* = 8.0, 2.1 Hz, 1H), 7.32 (dd, *J* = 8.0, 4.9 Hz, 1H), 6.40 (d, *J* = 7.9 Hz, 1H), 5.34 (s, 0H), 3.76 (dtt, *J* = 11.4, 8.5, 4.0 Hz, 1H), 3.61 (td, *J* = 5.6, 2.8 Hz, 1H), 3.20 (td, *J* = 5.7, 2.8 Hz, 1H), 3.05 – 2.97 (m, 1H), 2.95 – 2.87 (m, 1H), 1.94 – 1.83 (m, 2H), 1.73 – 1.55 (m, 2H), 1.43 – 1.26 (m, 3H), 1.22 – 0.98 (m, 4H). ^{13}C NMR (126 MHz, $CDCl_3$) δ 168.10, 166.82, 150.04, 149.62, 135.82, 130.98, 123.90, 58.10, 48.97, 39.28, 36.53, 32.89, 32.85, 29.84, 25.52, 24.82, 24.78.

2-((cyanomethyl)amino)-N-cyclohexyl-2-(pyridin-3-yl)acetamide (19). In a 6-dram vial equipped with a stir bar 3-Pyridinecarboxaldehyde (107 mg,1.0 mmol, 1.0 eq.) and b-alanine (89 mg, 1.0 mmol, 1.0 eq.) were mixed together in MeOH (4 mL).The obtained solution was stirred for 30 min. at room temperature. Cyclohexyl isocyanide (109 mg, 1.0 mmol, 1.0 eq.) was added to the reaction mixture and the walls of the vial were washed with 1 mL of MeOH. The obtained reaction mixture was stirred at room temperature overnight. The crude reaction mixture was evaporated in vacuo and redissolved in DCM. The obtained crude solution was deposited on silica. It was then purified using flash column chromatography using DCM/MeOH (gradient 0 → 5%) as eluent. The product was obtained as colorless oil, 156 mg 54%. ^{1}H NMR (500 MHz, $CDCl_3$) δ 8.65 (d, *J* = 2.4 Hz, 1H), 8.62 (dd, *J* = 4.8, 1.7 Hz, 1H), 7.75 (dt, *J* = 7.9, 2.0 Hz, 1H), 7.34 (dd, *J* = 7.9, 4.8 Hz, 1H), 6.02 (d, *J* = 8.4 Hz, 1H), 4.40 (s, 1H), 3.82 – 3.71 (m, 1H), 3.64 (d, *J* = 17.5 Hz, 1H), 3.45 (d, *J* = 17.3 Hz, 1H), 2.53 (s, 1H), 1.85 (ddd, *J* = 17.0, 12.4, 4.4 Hz, 2H), 1.64 (dtd, *J* = 25.9, 9.0, 4.7 Hz, 4H), 1.40 – 1.28 (m, 2H), 1.20 – 1.02 (m, 2H). ^{13}C NMR (126 MHz, $CDCl_3$) δ 168.45, 150.57, 149.43, 135.66, 133.25, 124.24, 116.87, 63.55, 48.67, 35.50,

33.06, 33.02, 25.49, 24.83. HRMS (ESI+) for $C_{15}H_{20}N_4NaO$ (M + Na) calculated 295.1529; found 295.1523.

(*E*)-*N*-(4-(*tert*-butyl)phenyl)-*N*-(2-(*tert*-butylamino)-2-oxo-1-(pyridin-3-yl)ethyl)but-2-enamide (21). Compound was purified using general procedure A, white solid 54 % yield, 198 mg. ^{1}H NMR (500 MHz, $CDCl_3$) δ 8.48 – 8.41 (m, 2H), 7.43 (d, J = 8.0 Hz, 1H), 7.26 (d, J = 8.2 Hz, 2H), 7.05 (dd, J = 8.0, 4.8 Hz, 1H), 7.01 – 6.95 (m, 1H), 6.91 (s, 1H), 6.35 (s, 1H), 6.07 (s, 1H), 5.68 (dd, J = 15.1, 1.7 Hz, 1H), 1.75 (dd, J = 7.1, 1.7 Hz, 3H), 1.39 (s, 9H), 1.30 (s, 9H).^{13}C NMR (126 MHz, $CDCl_3$) δ 168.38, 166.89, 151.78, 151.38, 149.47, 142.97, 138.10, 136.53, 130.94, 129.85, 126.20, 122.77, 63.16, 51.73, 34.76, 31.38, 28.81, 18.21. HRMS (ESI+) for $C_{25}H_{33}N_3NaO_2$ (M + Na) calculated 430.2438; found 430.2450.

***N*-(4-(*tert*-butyl)phenyl)-*N*-(2-(*tert*-butylamino)-2-oxo-1-(pyridin-3-yl)ethyl)but-2-ynamide (22).** Compound was purified using general procedure A, white solid 82 % yield, 300 mg. ^{1}H NMR (500 MHz, $CDCl_3$) δ 8.45 (dd, J = 4.8, 1.5 Hz, 1H), 8.43 (d, J = 2.3 Hz, 1H), 7.43 (dt, J = 8.1, 2.0 Hz, 1H), 7.25 – 7.20 (m, 2H), 7.05 (dd, J = 8.0, 4.8 Hz, 1H), 6.97 (d, J = 8.0 Hz, 2H), 6.09 (s, 1H), 5.96 (s, 1H), 1.68 (s, 3H), 1.36 (s, 9H), 1.26 (s, 9H). ^{13}C NMR (126 MHz, $CDCl_3$) δ 167.54, 155.43, 151.94, 151.27, 149.67, 138.25, 136.37, 130.29, 129.91, 125.77, 122.95, 92.21, 73.90, 62.66, 51.98, 34.76, 31.35, 28.75. HRMS (ESI+) for $C_{25}H_{31}N_3NaO_2$ (M + Na) calculated 428.2308; found 428.2307.

***N*-(4-(*tert*-butyl)phenyl)-*N*-(2-(*tert*-butylamino)-2-oxo-1-(pyridin-3-yl)ethyl)acrylamide (23).** Compound was purified using general procedure C, white solid 42 % yield, 150 mg. ^{1}H NMR (500 MHz, $CDCl_3$) δ 8.46 – 8.42 (m, 2H), 7.43 (dt, *J* = 8.0, 2.0 Hz, 1H), 7.24 (d, *J* = 8.3 Hz, 2H), 7.04 (ddd, *J* = 8.0, 4.9, 0.9 Hz, 1H), 6.91 (s, 1H), 6.40 (dd, *J* = 16.8, 2.0 Hz, 1H), 6.20 (s, 1H), 6.06 (s, 1H), 5.98 (dd, *J* = 16.8, 10.3 Hz, 1H), 5.55 (dd, *J* = 10.3, 2.0 Hz, 1H), 1.37 (s, 9H), 1.26 (s, 9H). ^{13}C NMR (126 MHz, $CDCl_3$) δ 168.13, 166.58, 152.00, 151.38, 149.58, 138.15, 136.19, 130.77, 129.89, 128.77, 128.60, 126.25, 122.87, 63.18, 51.84, 34.77, 31.37, 28.80. HRMS (ESI+) for $C_{24}H_{31}N_3NaO_2$ (M + Na) calculated 416.2308; found 416.2291.

***N*-(2-(cyclohexylamino)-2-oxo-1-(pyridin-3-yl)ethyl)-2-oxo-*N*-(m-tolyl)propanamide (24).** Compound was prepared according to the procedure for 13. Pale yellow solid, 134 mg, 37% yield. ^{1}H NMR (500 MHz, $CDCl_3$) δ 8.63 (d, *J* = 5.7 Hz, 2H), 7.69 (dd, *J* = 5.8, 3.8 Hz, 1H), 7.30 (dd, *J* = 8.0, 4.8 Hz, 1H), 7.25 – 7.14 (m, 2H), 7.07 (s, 1H), 7.02 (s, 1H), 6.22 (d, *J* = 8.0 Hz, 1H), 6.14 (s, 1H), 4.06 – 3.86 (m, 1H), 2.35 (s, 3H), 2.32 (s, 3H), 2.13 – 1.94 (m, 3H), 1.88 – 1.68 (m, 2H), 1.55 – 1.40 (m, 2H),

1.37 – 1.16 (m, 3H). ^{13}C NMR (126 MHz, $CDCl_3$) δ 197.36, 168.01, 166.76, 150.59, 149.11, 139.55, 138.91, 136.94, 130.81, 130.27, 130.10, 129.10, 127.29, 123.56, 62.46, 49.25, 32.88, 32.84, 27.84, 25.51, 24.88, 24.81, 21.22. HRMS (ESI+) for $C_{23}H_{27}N_3O_3$ (M + Na) calculated 416.1945; found 416.1952

***N*-(4-(*tert*-butyl)phenyl)-*N*-(2-(cyclohexylamino)-2-oxo-1-(thiophen-3-yl)ethyl)cyclopent-1-ene-1-carboxamide (25).** Compound was purified using general procedure B, off white solid 79 % yield, 330 mg. ^{1}H NMR (500 MHz, $CDCl_3$) δ 7.27 – 7.24 (m, 1H), 7.20 – 7.12 (m, 3H), 6.94 – 6.87 (m, 3H), 6.09 (d, *J* = 8.1 Hz, 1H), 6.06 (s, 1H), 5.81 (q, *J* = 2.2 Hz, 1H), 3.87 – 3.76 (m, 1H), 2.22 – 2.06 (m, 4H), 2.01 – 1.84 (m, 2H), 1.71 – 1.53 (m, 5H), 1.42 – 1.28 (m, 2H), 1.26 (s, 9H), 1.15 (ddt, *J* = 16.1, 12.0, 8.0 Hz, 3H). ^{13}C NMR (126 MHz, $CDCl_3$) δ 168.73, 168.53, 151.12, 139.46, 139.40, 138.34, 135.52, 129.16, 129.08, 126.40, 125.51, 125.33, 61.62, 48.59, 34.68, 33.83, 33.19, 32.97, 32.93, 31.42, 25.67, 24.88, 24.83, 23.36. HRMS (ESI+) for $C_{28}H_{36}N_2NaO_2S$ (M + Na) calculated 487.2390; found 487.2404.

***N*-(4-(*tert*-butyl)phenyl)-*N*-(2-(cyclohexylamino)-2-oxo-1-(quinolin-3-yl)ethyl)cyclopent-1-ene-1-carboxamide (26).** Compound was purified using general procedure B, pale yellow solid 59 % yield, 270 mg. H NMR (500 MHz, $CDCl_3$) δ 8.73 (d, *J* = 2.1 Hz, 1H), 8.03 (d, *J* = 8.4 Hz, 1H), 8.00 (s, 1H), 7.74 – 7.66 (m, 1H), 7.65 – 7.61 (m, 1H), 7.52 – 7.45 (m, 1H), 7.13 (d, *J* = 8.2 Hz, 2H), 6.39 (s, 2H), 6.27 (s, 1H), 5.86 (p, *J* = 2.3 Hz, 1H), 3.93 – 3.82 (m, 1H), 2.23 – 2.09 (m, 4H), 2.00 (dd, *J* = 12.2, 4.1 Hz, 2H), 1.89 (dd, *J* = 12.8, 4.2 Hz, 1H), 1.66 (p, *J* = 7.7 Hz, 5H), 1.36 (ddd, *J* = 16.2, 13.1, 11.4 Hz, 2H), 1.19 (s, 9H), 1.18 – 1.08 (m, 3H). ^{13}C NMR (126 MHz, $CDCl_3$) δ 169.02, 168.29, 151.91, 151.58, 147.65, 140.28, 139.13, 138.06, 137.59, 130.00, 129.59, 129.15, 128.23, 127.98, 127.47, 126.87, 125.83, 63.71, 48.83, 34.69, 33.87, 33.26, 33.02, 32.98, 31.31, 25.62, 24.90, 24.85, 23.32. HRMS (ESI+) for $C_{33}H_{39}N_3NaO_2$ (M + Na) calculated 532.2934; found 532.2946.

***N*-(1-(benzo[b]thiophen-3-yl)-2-(cyclohexylamino)-2-oxoethyl)-*N*-(4-(*tert*-butyl)phenyl)cyclopent-1-ene-1-carboxamide (27).** Compound was purified using general procedure B, pale yellow solid 26 % yield, 120 mg. ^{1}H NMR (500 MHz, $CDCl_3$) δ 7.83 (d, *J* = 7.6 Hz, 1H), 7.78 – 7.72 (m, 1H), 7.53 (s, 1H), 7.37 (p, *J* = 7.0 Hz, 2H), 7.03 (d, *J* = 8.2 Hz, 2H), 6.69 (d, *J* = 19.7 Hz, 3H), 6.20 (d, *J* = 8.2 Hz, 1H), 5.84 – 5.79 (m, 1H), 2.17 – 2.00 (m, 4H), 1.97 – 1.90 (m, 2H), 1.65 (pt, *J* = 14.3, 6.5 Hz, 5H), 1.36 (ddt, *J* = 15.3, 11.9, 6.0 Hz, 3H), 1.19 (s, 12H). ^{13}C NMR (126 MHz, $CDCl_3$) δ 169.16, 168.29, 151.15, 139.68, 139.60, 139.30, 138.74, 137.04, 129.40, 129.26, 129.10, 125.16, 124.61,

124.59, 122.92, 121.61, 57.25, 48.65, 34.61, 33.87, 33.18, 33.04, 32.98, 31.36, 25.65, 24.94, 24.89, 23.36. HRMS (ESI+) for $C_{32}H_{38}N_2NaO_2S$ (M + Na) calculated 537.2546; found 537.2549.

***N*-(4-(*tert*-butyl)phenyl)-*N*-(2-(cyclohexylamino)-2-oxo-1-(pyridin-4-yl)ethyl)cyclopent-1-ene-1-carboxamide (28).** Compound was purified using general procedure B, white solid 371 % yield, 90 mg. ^{1}H NMR (500 MHz, $CDCl_3$) δ 8.49 (d, *J* = 6.2 Hz, 2H), 7.30 – 7.19 (m, 4H), 6.97 (d, *J* = 8.1 Hz, 2H), 6.45 (d, *J* = 8.1 Hz, 1H), 5.88 (p, *J* = 2.2 Hz, 1H), 5.82 (s, 1H), 3.89 – 3.78 (m, 1H), 2.21 (ddt, *J* = 7.6, 5.0, 2.6 Hz, 2H), 2.12 (dtt, *J* = 9.9, 5.0, 2.2 Hz, 2H), 1.98 – 1.84 (m, 3H), 1.67 (p, *J* = 7.4 Hz, 4H), 1.43 – 1.29 (m, 2H), 1.26 (s, 9H), 1.19 (dddd, *J* = 26.8, 22.7, 10.8, 4.5 Hz, 3H). ^{13}C NMR (126 MHz, $CDCl_3$) δ 169.03, 167.76, 151.65, 149.80, 144.29, 140.77, 139.08, 138.60, 128.71, 126.05, 124.23, 67.01, 48.74, 34.76, 33.69, 33.27, 32.92, 32.88, 31.39, 25.62, 24.80, 23.34.

***N*-(4-(*tert*-butyl)phenyl)-*N*-(2-(cyclohexylamino)-2-oxo-1-(pyrimidin-5-yl)ethyl)cyclopent-1-ene-1-carboxamide (29).** Compound was purified using general procedure B, off white solid 29 % yield, 120 mg. ^{1}H NMR (500 MHz, $CDCl_3$) δ 9.06 (s, 1H), 8.55 (s, 2H), 7.25 (d, *J* = 8.9 Hz, 2H), 6.85 (dd, *J* = 15.8, 5.0 Hz, 2H), 6.62 (d, *J* = 8.1 Hz, 1H), 6.18 (s, 1H), 5.84 (td, *J* = 2.7, 1.3 Hz, 1H), 3.89 – 3.78 (m, 1H), 2.55 (dd, *J* = 25.2, 2.4 Hz, 2H), 2.20 (ddd, *J* = 7.8, 6.0, 2.5 Hz, 2H), 2.12 (ddd, *J* = 10.3, 5.6, 2.3 Hz, 2H), 2.01 – 1.86 (m, 1H), 1.76 – 1.57 (m, 5H), 1.46 – 1.31 (m, 2H), 1.27 (s, 9H), 1.26 – 1.14 (m, 3H). ^{13}C NMR (101 MHz, $CDCl_3$) δ 169.14, 167.31, 158.59, 158.11, 152.37, 145.94, 141.02, 138.68, 136.78, 129.38, 128.84, 126.31, 61.37, 48.85, 34.82, 33.84, 33.70, 33.32, 32.99, 32.91, 31.36, 31.32, 25.60, 24.79, 23.31, 23.29. HRMS (ESI+) for $C_{28}H_{36}N_4NaO_2$ (M + Na) calculated 483.2730; found 483.2746.

***N*-(4-(*tert*-butyl)phenyl)-*N*-(2-(cyclohexylamino)-1-(isoquinolin-4-yl)-2-oxoethyl)cyclopent-1-ene-1-carboxamide (30).** Compound was purified using general procedure A, off white solid 78 % yield, 358 mg. ^{1}H NMR (500 MHz, $CDCl_3$) δ 9.08 (d, *J* = 1.9 Hz, 1H), 8.28 (s, 1H), 8.01 (d, *J* = 8.5 Hz, 1H), 7.95 (d, *J* = 8.1 Hz, 1H), 7.77 (dd, *J* = 8.5, 6.9 Hz, 1H), 7.66 – 7.59 (m, 1H), 7.06 (s, 1H), 6.93 (d, *J* = 8.1 Hz, 2H), 6.78 (s, 1H), 5.81 (q, *J* = 2.1 Hz, 1H), 5.67 (s, 1H), 3.91 (dt, *J* = 7.5, 3.5 Hz, 1H), 2.21 – 2.09 (m, 4H), 1.97 (d, *J* = 16.2 Hz, 2H), 1.72 – 1.62 (m, 5H), 1.34 (tdd, *J* = 12.3, 8.3, 3.8 Hz, 2H), 1.13 (d, *J* = 0.9 Hz, 12H). ^{13}C NMR (126 MHz, $CDCl_3$) δ 168.96, 168.39, 153.31, 151.05, 145.51, 139.71, 139.19, 136.80, 135.07, 131.47, 129.61, 128.57, 128.14, 127.44, 125.06, 124.84, 122.71, 58.84, 49.11, 34.52, 33.87, 33.23, 33.04, 33.00, 31.28, 25.61, 25.00, 24.89, 23.34. HRMS (ESI+) for $C_{33}H_{39}N_3NaO_2$ (M + Na) calculated 532.2934; found 532.2932.

***N*-(4-(*tert*-butyl)phenyl)-*N*-(2-(tert-butylamino)-2-oxo-1-(pyridin-3-yl)ethyl)furan-2-carboxamide (31).** Compound was purified using general procedure A, white solid 84 % yield, 290 mg. ^{1}H NMR (500 MHz, $CDCl_3$) δ 8.48 (d, *J* = 2.3 Hz, 1H), 8.46 (dd, *J* = 4.9, 1.7 Hz, 1H), 7.51 (d, *J* = 8.1 Hz, 1H), 7.39 (dd, *J* = 1.7, 0.7 Hz, 1H), 7.24 (d, *J* = 6.6 Hz, 2H), 7.06 (ddd, *J* = 8.0, 4.8, 0.8 Hz, 1H), 6.98 (s, 2H), 6.19 – 6.13 (m, 2H), 6.10 (s, 1H), 5.38 (dd, *J* = 3.6, 0.8 Hz, 1H), 1.37 (s, 9H), 1.28 (s, 9H). ^{13}C NMR (126 MHz, $CDCl_3$) δ 167.96, 159.80, 152.62, 151.59, 149.72, 146.36, 145.12, 138.32, 136.63, 130.56, 130.30, 126.22, 122.94, 117.26, 111.35, 63.83, 51.92, 34.84, 31.41, 28.80. $C_{26}H_{31}N_3NaO_3$ (M + Na) calculated 456.2258; found 456.2245.

(*E*)-*N*-(4-(*tert*-butyl)phenyl)-*N*-(2-(cyclohexylamino)-2-oxo-1-(pyridin-4-yl)ethyl)but-2-enamide (32). Compound was purified using general procedure A, white solid 74 % yield, 287 mg. ^{1}H NMR (500 MHz, $CDCl_3$) δ 8.49 – 8.45 (m, 2H), 7.28 (d, *J* = 8.9 Hz, 2H), 7.19 – 7.12 (m, 2H), 7.03 – 6.92 (m, 3H), 6.47 (d, *J* = 7.9 Hz, 1H), 5.84 (s, 1H), 5.70 (dd, *J* = 15.0, 1.8 Hz, 1H), 4.03 – 3.75 (m, 1H), 1.95 (dd, *J* = 12.3, 4.3 Hz, 1H), 1.91 – 1.85 (m, 1H), 1.78 – 1.74 (m, 3H), 1.70 – 1.64 (m, 2H), 1.58 (dt, *J* = 12.9, 3.9 Hz, 1H), 1.37 – 1.31 (m, 2H), 1.29 (s, 9H), 1.25 – 1.08 (m, 3H). ^{13}C NMR (126 MHz, $CDCl_3$) δ 167.84, 167.10, 151.87, 149.73, 144.20, 143.48, 137.54, 129.06, 126.42, 124.35, 122.64, 66.12, 48.75, 34.80, 32.89, 31.39, 25.62, 24.83, 24.80, 18.25. HRMS (ESI+) for $C_{27}H_{35}N_3NaO_2$ (M + Na) calculated 456.2621; found 456.2614.

***N*-(*tert*-butyl)-2-(*N*-(4-(*tert*-butyl)phenyl)acetamido)-2-(pyridin-3-yl)acetamide (33).** Compound was purified using general procedure A, white solid 84 % yield, 290 mg. ^{1}H NMR (500 MHz, $CDCl_3$) δ 8.43 (dd, *J* = 4.8, 1.6 Hz, 1H), 8.40 (s, 1H), 7.37 (d, *J* = 8.1 Hz, 1H), 7.22 (d, *J* = 8.2 Hz, 2H), 7.01 (dd, *J* = 7.6, 5.3 Hz, 1H), 6.91 (s, 1H), 6.04 (s, 1H), 5.98 (s, 1H), 1.87 (s, 3H), 1.36 (s, 9H), 1.25 (s, 9H). ^{13}C NMR (126 MHz, $CDCl_3$) δ 171.75, 168.32, 151.86, 151.45, 149.59, 138.13, 137.31, 130.88, 129.65, 126.24, 122.84, 62.64, 51.80, 34.72, 31.36, 28.79, 23.36. HRMS (ESI+) for $C_{23}H_{31}N_3NaO_2$ (M + Na) calculated 404.2308; found 404.2307.

***N*-(4-(*tert*-butyl)phenyl)-2-chloro-*N*-(2-(cyclohexylamino)-2-oxo-1-(thiophen-3-yl)ethyl)acetamide (34).** Compound was purified using general procedure A, white solid 87 % yield, 352 mg. ^{1}H NMR (500 MHz, $CDCl_3$) δ 7.28 (s, 2H), 7.25 – 7.21 (m, 1H), 7.17 (dd, *J* = 5.0, 3.0 Hz, 1H), 6.84 (dd, *J* = 5.0, 1.3 Hz, 1H), 6.01 (s, 1H), 5.79 (d, *J* = 8.2 Hz, 1H), 3.87 (s, 2H), 3.82 (ddt, *J* = 14.7, 6.7, 3.9 Hz, 1H), 1.98 – 1.92 (m, 1H), 1.91 – 1.85 (m, 1H), 1.74 – 1.60 (m, 3H), 1.38 (dqd, *J* = 8.3, 3.3, 1.6 Hz, 2H), 1.30 (s, 9H), 1.23 – 1.05 (m, 3H). ^{13}C NMR (126 MHz, $CDCl_3$) δ 167.83, 166.99, 152.39,

136.30, 134.59, 129.25, 128.85, 126.93, 126.34, 125.82, 61.28, 48.89, 42.69, 34.81, 32.95 (d, *J* = 10.4 Hz),31.57, 31.38, 25.62, 24.90, 24.84.

***N*-(4-(*tert*-butyl)phenyl)-2-chloro-*N*-(2-(cyclohexylamino)-2-oxo-1-(pyridin-4-yl)ethyl)acetamide (35).** Compound was purified using general procedure A, white solid 94 % yield, 375 mg. ^{1}H NMR (500 MHz, $CDCl_3$) δ 8.47 (d, *J* = 6.1 Hz, 2H), 7.26 (s, 2H), 7.16 – 7.11 (m, 2H), 5.88 (d, *J* = 8.0 Hz, 1H), 5.83 (s, 1H), 3.87 (d, *J* = 1.9 Hz, 2H), 3.85 – 3.77 (m, 1H), 2.00 – 1.94 (m, 1H), 1.86 (dd, *J* = 12.9, 4.0 Hz, 1H), 1.75 – 1.53 (m, 3H), 1.41 – 1.28 (m, 2H), 1.26 (s, 9H), 1.23 – 1.03 (m, 3H). ^{13}C NMR (126 MHz, $CDCl_3$) δ 167.57, 166.93, 152.92, 149.88, 143.19, 135.93, 129.26, 126.68, 124.90, 65.47, 49.11, 42.49, 34.87, 32.90, 32.85, 31.33, 25.56, 24.88, 24.82.

***N*-(4-(tert-butyl)phenyl)-*N*-(2-(cyclopentylamino)-2-oxo-1-(pyridin-3-yl)ethyl)but-2-ynamide (36).** Compound was purified using general procedure A, white solid 94 % yield, 354 mg. ^{1}H NMR (500 MHz, $CDCl_3$) δ 8.46 (dd, *J* = 4.9, 1.6 Hz, 1H), 8.44 (d, *J* = 2.3 Hz, 1H), 7.50 – 7.44 (m, 1H), 7.23 (d, *J* = 8.8 Hz, 2H), 7.07 (dd, *J* = 8.0, 4.8 Hz, 1H), 6.97 (d, *J* = 8.0 Hz, 2H), 6.20 (s, 1H), 6.02 (s, 1H), 4.23 (h, *J* = 6.8 Hz, 1H), 2.02 (dd, *J* = 13.0, 6.2 Hz, 1H), 1.95 (q, *J* = 2.7 Hz, 1H), 1.68 (s, 3H), 1.64 – 1.56 (m, 4H), 1.49 – 1.42 (m, 1H), 1.39 – 1.34 (m, 1H), 1.26 (s, 9H). ^{13}C NMR (126 MHz, $CDCl_3$) δ 167.92, 155.47, 151.97, 151.06, 149.54, 138.34, 136.39, 130.32, 129.87, 125.79, 123.06, 92.26, 73.85, 62.23, 51.89, 34.76, 33.08, 33.01, 31.34, 23.87, 23.84, 4.06.

***N*-(2-(benzylamino)-2-oxo-1-(pyridin-3-yl)ethyl)-*N*-(4-(tert-butyl)phenyl)but-2-ynamide (37).** Compound was purified using general procedure A, pale yellow solid 86 % yield, 340 mg. ^{1}H NMR (500 MHz, $CDCl_3$) δ 8.43 (d, *J* = 4.7 Hz, 1H), 8.40 (t, *J* = 1.6 Hz, 2H), 7.45 (d, *J* = 7.8 Hz, 1H), 7.33 – 7.16 (m, 6H), 7.05 (dd, *J* = 8.0, 4.8 Hz, 1H), 6.94 (d, *J* = 8.1 Hz, 2H), 6.66 (d, *J* = 8.5 Hz, 1H), 6.05 (s, 1H), 4.55 – 4.43 (m, 2H), 1.66 (s, 3H), 1.25 (s, 9H). ^{13}C NMR (126 MHz, $CDCl_3$) δ 168.38, 155.47, 151.96, 151.08, 149.59, 138.41, 137.91, 136.33, 130.18, 129.93, 128.85, 127.84, 127.64, 125.78, 123.11, 92.27, 73.83, 62.35, 44.02, 34.74, 31.65, 31.33, 4.04.

***N*-(4-(*tert*-butyl)phenyl)-2-chloro-*N*-(2-(cyclopentylamino)-2-oxo-1-(pyridin-3-yl)ethyl)acetamide (38).** Compound was purified using general procedure A, pale yellow solid 88 % yield, 340 mg. ^{1}H NMR (500 MHz, $CDCl_3$) δ 8.46 (dd, *J* = 4.9, 1.7 Hz, 1H), 8.42 (d, *J* = 2.3 Hz, 1H), 7.44 (dd, *J* = 8.0, 2.1 Hz, 1H), 7.26 (s, 3H), 7.06 (dd, *J* = 8.0, 4.8 Hz, 1H), 6.06 (d, *J* = 7.3 Hz, 1H), 5.99 (s, 1H), 4.23 (h, *J* = 6.8 Hz, 1H), 3.85 (s, 2H), 2.10 – 1.99 (m, 1H), 1.98 – 1.90 (m, 1H), 1.70 – 1.52 (m, 4H), 1.51 – 1.40 (m, 1H), 1.33 (dq, *J* = 13.6, 6.8, 5.8 Hz, 1H), 1.25 (s, 9H). ^{13}C NMR (126 MHz,

$CDCl_3$) δ 167.93, 167.42, 152.82, 151.20, 149.68, 138.30, 135.29, 130.25, 129.75, 126.59, 123.16, 63.03, 51.94, 42.61, 34.83, 33.08, 33.03, 31.32, 23.88, 23.86.

***N*-benzyl-2-(*N*-(4-(*tert*-butyl)phenyl)-2-chloroacetamido)-2-(pyridin-3-yl)acetamide (39).** Compound was purified using general procedure A, yellow solid 91 % yield, 370 mg. ^{1}H NMR (500 MHz, $CDCl_3$) δ 8.45 (dd, *J* = 4.8, 1.6 Hz, 1H), 8.40 (d, *J* = 2.3 Hz, 1H), 7.43 (dt, *J* = 8.0, 2.1 Hz, 1H), 7.35 – 7.13 (m, 9H), 7.04 (ddd, *J* = 8.1, 4.9, 0.9 Hz, 1H), 6.55 (s, 1H), 6.06 (s, 1H), 4.49 (qd, *J* = 14.8, 5.8 Hz, 2H), 3.85 (d, *J* = 1.5 Hz, 2H), 1.25 (s, 9H). ^{13}C NMR (126 MHz, $CDCl_3$) δ 168.45, 167.46, 152.84, 151.36, 149.93, 138.24, 137.84, 135.18, 129.95, 129.79, 128.86, 127.83, 127.70, 126.59, 123.14, 63.10, 44.07, 42.67, 34.82, 31.31.

***N*-(4-(*tert*-butyl)phenyl)-2-chloro-*N*-(2-(cyclohexylamino)-1-(5-methylpyrazin-2-yl)-2-oxoethyl)acetamide (40).** Compound was purified using general procedure B, pale yellow solid 34 % yield, 140 mg. ^{1}H NMR (500 MHz, $CDCl_3$) δ 8.62 (s, 1H), 8.39 (s, 1H), 7.37 (d, *J* = 8.2 Hz, 2H), 7.29 – 7.06 (m, 2H), 5.88 (s, 1H), 3.89 (q, *J* = 13.6 Hz, 2H), 3.82 – 3.72 (m, 1H), 1.92 – 1.85 (m, 3H), 1.77 – 1.53 (m, 5H), 1.32 (s, 13H), 1.22 – 1.12 (m, 2H). ^{13}C NMR (126 MHz, $CDCl_3$) δ 167.11, 165.73, 153.11, 152.59, 147.62, 144.81, 142.87, 136.87, 128.87, 126.66, 65.99, 48.50, 42.31, 34.75, 32.59, 32.49, 31.60, 31.24, 25.48, 24.57, 24.50, 22.66, 21.31, 14.13.

***In vitro* assays.**

Protein production. Based on Zhang *et al.* methodology,[38] the DNA sequence encoding 3CL SARS-CoV-2 protease (GI: 1831502838) was synthetized (optimized for *Escherichia coli* expression) and then cloned into a pGEX-6-1 vector between BamHI and XhoI restriction sites, by GenScript (Piscataway, NJ, USA). In the plasmid, the protein sequence was preceded by the N-terminal GST sequence (and the HRV3C site, for PreScission protease) and it starts as follow: SAVLQ↓SGFRK. The autocleavage activity of the enzyme leaves its N-terminus starting in the serine after the QS cleavage site (Q↓S). At the C-terminus, based on Xue *et al.*,[39] and Zhang *et al.*[38]), the protein was designed to end with the last glutamine (the natural C-terminus of the enzyme) if needed. By adding a glycine and a proline residue after the last glutamine, followed by six histidine residues, the protein obtains the modified-PreScission (approach developed Xue *et al.*,[39] for the SARS-CoV 3CL^{pro}) SGVTFQ↓GP and a six-histidine-tag (HisTag).

E. coli BL21 (DE3) cells were transformed using the described construct and colonies selected on LB-agar-ampicillin plates. A single colony was picked and grew over night in LB medium and then used for inoculating a 400 mL LB culture. This culture was gown at 37 ºC, 250 rpm, until 0.7 absorbance (O.D.600) is reached and then induced during 18h at 16 ºC (250 rpm) adding 0.25 mM IPTG. The bacterial pellet was collected after 4,000 rpm centrifugation and resuspended in 30 mL of 50 mM Tris-HCl pH 8.0, 150 mM NaCl (resuspension buffer). An Ultrasonic Cell Disruption Sonifier 450 (Branson) was used to sonicate the cells (on ice) with 6 pulses of 2 minutes (7 of Output Control and 50 % of Duty Cycle).

Buffer A (50 mM Tris-HCl pH 8.0, 150 mM NaCl, 20 mM imidazole) and Buffer B (50 mM Tris-HCl, 150 mM NaCl, 500 mM imidazole) were used for purifying 3CL^{pro} after the clarified supernatant (14,000 rpm centrifugation) was loaded into a 1 mL HisTrap FF (GE Healthcare, IL, USA). 5 mL fractions were collected in single steps of column washing increasing imidazole concentration (0, 5, 10, 15, 20, 25, 30, 35, 40, 45 and 50 % Buffer B).

After running SDS-PAGE for confirmation (Mini-PROTEAN® TGX™ Precast Gels, Bio-Rad), two sets of fractions were pooled independently (then re-ran into a protein gel). One of them, contains the target enzyme, but contaminated with a high molecular weight protein (5 and 10 % Buffer B) and the other only the pure enzyme (15, 20 and 25 % buffer B). Imidazole was eliminated from pooled fractions by washing them multiple times (with resuspension buffer) using 10K cut-off Amicon® Ultra-15 Centrifugal Filter Units (Millipore Sigma, Burlington, MA, USA). Absorbance at 280 nm was recorded for the pure sample and the protein concentration was estimated to be 8.5 µM (around 0.3 g/L); based on SDS-PAGE results, the same concentration was assumed for the other sample. These samples were aliquoted and stored at -20 Celsius degrees. In all the experiments (unless specified) the pure preparation was used. See Figure S1 for more information.

Detection of inhibitors by fluorescence spectrophotometry. For all inhibition experiments, a 50 µL assay was established using 11.76 µM fluorescence substrate DABCYL-KTSAVLQSGFRKME-EDANS from BPS Biosciences (San Diego, CA, USA). This substrate has been regularly used for assaying 3CL proteases.[40]

38 µL of enzyme (diluted in a 3CL^{pro} Protease Assay Buffer from BPS Bioscience supplemented with 1 mM DTT) were incubated, between 20 to 40 minutes at room temperature, with 2 µL of 1.25 mM compounds (diluted in DMSO; Sigma). In both cases, screenings (duplicates) and IC_{50} experiments

(duplicates and triplicates), 10 µL of diluted substrate (58.8 µM) were added and reactions recorded following fluorescence increase in time (excitation at 360 nm, emission at 460 nm) using a Synergy™ H4 Hybrid Multi-Mode Microplate Reader (Winooski, VT, USA). Each figure legend reports the enzyme concentration used (between 80 to 240 nM). Controls were (i) no inhibition, only DMSO, and (ii) positive inhibition, compound GC376 (BPS Bioscience) diluted in distillate water. In all cases the compounds were added as DMSO solutions and their final concentration in the screenings was 50 µM. The reactions were run for at least one hour (to see the plateau of maximum velocity), and the linear section of the progress curves were selected for calculating initial velocity in Relative Fluorescent Units in time (RFU per minute).

Liquid chromatography-mass spectrometry (LC-MS). Frozen-stored protein was buffer exchanged with 5 mM Tris-HCl pH 8.0, 15 mM NaCl buffer using 4K cut-off Amicon® small Centrifugal Filter Units (Millipore Sigma, Burlington, MA, USA) and prepared at 0.1-0.2 mg/mL. 96 µL of this solution were mixed with 4 µL of 2.5 mM **4** or **15**. Pure DMSO was used as a negative control. Every 20 minutes 10 µL of these solutions were injected into a Dionex Ultimate 3000 UHPLC coupled to a Bruker Maxis Impact QTOF in positive ESI mode.

Isothermal Titration Calorimetry (ITC). All ITC experiments were performed on a Malvern ITC200 instrument in high-feedback mode with a 5s signal averaging window, a stirring rate of 750 rpm, pre-injection delay of 60 s, and a reference power of 7. A first small injection of 0.2 µL was used to prevent errors arising from syringe diffusion followed by experiments five sequential 7 µL injections with a wait period of 180 seconds. Experiments were ran using 1mM peptide Cbz-TSAVLQSGFRK order from CanPeptide, 8.5 µM 3CL^{pro}, and 10µM **15** when required. All compounds were dissolved in a 50 mM Tris-HCl pH 8.0, 150 mM NaCl buffer containing 4% DMSO and 5 mM TCEP.

Supporting Information

Addition information on LC-MS data, ITC measurement, dose-response curves and ^{1}H and ^{13}C NMR spectra.

Author information

Felipe A. Venegas' current address: Centre for Structural and Functional Genomics and Department of Chemistry and Biochemistry, Concordia University, 7141 Sherbrooke Street West, Montreal, QC, H4B 1R6, Canada

Acknowledgment

We thank the Canadian Institutes of Health Research (CIHR, OV3-170644), the McGill Interdisciplinary Initiative in Infection and Immunity (MI4) and the Faculty of Science for funding. We thank Dr. Alex Wahba for assistance with the LC/MS experiments.

References

(1) https://www.who.int/csr/sars/country/table2004_04_21/en/.
(2) https://www.ecdc.europa.eu/en/publications-data/distribution-confirmed-cases-mers-cov-place-infection-and-month-onset-march-2012.
(3) Schlottau, K.; Rissmann, M.; Graaf, A.; Schön, J.; Sehl, J.; Wylezich, C.; Höper, D.; Mettenleiter, T. C.; Balkema-Buschmann, A.; Harder, T.; Grund, C.; Hoffmann, D.; Breithaupt, A.; Beer, M. SARS-CoV-2 in fruit bats, ferrets, pigs, and chickens: an experimental transmission study. *Lancet Micr.* **2020**, *1*, E218-E225.
(4) Shi, Z.; Hu, Z. A review of studies on animal reservoirs of the SARS coronavirus. *Virus Res.* **2008**, *133*, 74-87.
(5) https://www.imperial.ac.uk/mrc-global-infectious-disease-analysis/news--wuhan-coronavirus/.
(6) WHO Coronavirus Disease (COVID-19) Dashboard. https://covid19.who.int/ (accessed Oct, 7 2020).
(7) Wu, A.; Peng, Y.; Huang, B.; Ding, X.; Wang, X.; Niu, P.; Meng, J.; Zhu, Z.; Zhang, Z.; Wang, J.; Sheng, J.; Quan, L.; Xia, Z.; Tan, W.; Cheng, G.; Jiang, T. Genome Composition and Divergence of the Novel Coronavirus (2019-nCoV) Originating in China. *Cell Host & Microbe* **2020**.
(8) Rathnayake, A. D.; Kim, Y.; Dampalla, C. S.; Nguyen, H. N.; Jesri, A.-R. M.; Kashipathy, M. M.; Lushington, G. H.; Battaile, K. P.; Lovell, S.; Chang, K.-O.; Groutas, W. C. Structure-Guided Optimization of Dipeptidyl Inhibitors of Norovirus 3CL Protease. *J. Med. Chem.* **2020**.
(9) Kuo, C.-J.; Shie, J.-J.; Fang, J.-M.; Yen, G.-R.; Hsu, J. T. A.; Liu, H.-G.; Tseng, S.-N.; Chang, S.-C.; Lee, C.-Y.; Shih, S.-R.; Liang, P.-H. Design, synthesis, and evaluation of 3C protease inhibitors as anti-enterovirus 71 agents. *Bioorg. Med. Chem.* **2008**, *16*, 7388-7398.
(10) Dragovich, P. S.; Prins, T. J.; Zhou, R.; Webber, S. E.; Marakovits, J. T.; Fuhrman, S. A.; Patick, A. K.; Matthews, D. A.; Lee, C. A.; Ford, C. E.; Burke, B. J.; Rejto, P. A.; Hendrickson, T. F.; Tuntland, T.; Brown, E. L.; Meador, J. W.; Ferre, R. A.; Harr, J. E. V.; Kosa, M. B.; Worland, S. T. Structure-Based Design, Synthesis, and Biological Evaluation of Irreversible Human Rhinovirus 3C Protease Inhibitors. 4. Incorporation of P1 Lactam Moieties as l-Glutamine Replacements. *J. Med. Chem.* **1999**, *42*, 1213-1224.
(11) Pillaiyar, T.; Manickam, M.; Namasivayam, V.; Hayashi, Y.; Jung, S.-H. An Overview of Severe Acute Respiratory Syndrome–Coronavirus (SARS-CoV) 3CL Protease Inhibitors: Peptidomimetics and Small Molecule Chemotherapy. *J. Med. Chem.* **2016**, *59*, 6595-6628.
(12) Anand, K.; Ziebuhr, J.; Wadhwani, P.; Mesters, J. R.; Hilgenfeld, R. Coronavirus Main Proteinase (3CLpro) Structure: Basis for Design of Anti-SARS Drugs. *Science* **2003**, *300*, 1763-1767.
(13) Liu, C.; Zhou, Q.; Li, Y.; Garner, L. V.; Watkins, S. P.; Carter, L. J.; Smoot, J.; Gregg, A. C.; Daniels, A. D.; Jervey, S.; Albaiu, D. Research and Development on Therapeutic Agents and Vaccines for COVID-19 and Related Human Coronavirus Diseases. *ACS Cent. Sci.* **2020**, *6*, 315-331.

(14) Westberg, M.; Su, Y.; Zou, X.; Ning, L.; Hurst, B.; Tarbet, B.; Lin, M. Z. Rational design of a new class of protease inhibitors for the potential treatment of coronavirus diseases. *bioRxiv* **2020**, 2020.2009.2015.275891.

(15) Iketani, S.; Forouhar, F.; Liu, H.; Hong, S. J.; Lin, F.-Y.; Nair, M. S.; Zask, A.; Huang, Y.; Xing, L.; Stockwell, B. R.; Chavez, A.; Ho, D. D. Lead compounds for the development of SARS-CoV-2 3CL protease inhibitors. *bioRxiv* **2020**, 2020.2008.2003.235291.

(16) Boras, B.; Jones, R. M.; Anson, B. J.; Arenson, D.; Aschenbrenner, L.; Bakowski, M. A.; Beutler, N.; Binder, J.; Chen, E.; Eng, H.; Hammond, J.; Hoffman, R.; Kadar, E. P.; Kania, R.; Kimoto, E.; Kirkpatrick, M. G.; Lanyon, L.; Lendy, E. K.; Lillis, J. R.; Luthra, S. A.; Ma, C.; Noell, S.; Obach, R. S.; O' Brien, M. N.; O'Connor, R.; Ogilvie, K.; Owen, D.; Pettersson, M.; Reese, M. R.; Rogers, T. F.; Rossulek, M. I.; Sathish, J. G.; Steppan, C.; Ticehurst, M.; Updyke, L. W.; Zhu, Y.; Wang, J.; Chatterjee, A. K.; Mesecar, A. D.; Anderson, A. S.; Allerton, C. Discovery of a Novel Inhibitor of Coronavirus 3CL Protease as a Clinical Candidate for the Potential Treatment of COVID-19. *bioRxiv* **2020**, 2020.2009.2012.293498.

(17) Hoffman, R.; Kania, R. S.; Brothers, M. A.; Davies, J. F.; Ferre, R. A.; Gajiwala, K. S.; He, M.; Hogan, R. J.; Kozminski, K.; Li, L. Y.; Lockner, J. W.; Lou, J.; Marra, M. T.; Mitchell, L. J. J.; Murraya, B. W.; Nieman, J. A.; Noell, S.; Planken, S. P.; Rowe, T.; Ryan, K.; Smith, G. J. I.; Solowiej, J. E.; Steppan, C. M.; Taggart, B. The Discovery of Ketone-Based Covalent Inhibitors of Coronavirus 3CL Proteases for the Potential Therapeutic Treatment of COVID-19. *ChemRxiv* **2020**, *https://doi.org/10.26434/chemrxiv.12631496.v1*

(18) Halford, B. Pfizer's novel COVID-19 antiviral heads to clinical trials. *C&EN* **2020**, *Sept 17*.

(19) Drayman, N.; Jones, K. A.; Azizi, S.-A.; Froggatt, H. M.; Tan, K.; Maltseva, N. I.; Chen, S.; Nicolaescu, V.; Dvorkin, S.; Furlong, K.; Kathayat, R. S.; Firpo, M. R.; Mastrodomenico, V.; Bruce, E. A.; Schmidt, M. M.; Jedrzejczak, R.; Muñoz-Alía, M. Á.; Schuster, B.; Nair, V.; Botten, J. W.; Brooke, C. B.; Baker, S. C.; Mounce, B. C.; Heaton, N. S.; Dickinson, B. C.; Jaochimiak, A.; Randall, G.; Tay, S. Drug repurposing screen identifies masitinib as a 3CLpro inhibitor that blocks replication of SARS-CoV-2 in vitro. *bioRxiv* **2020**, 2020.2008.2031.274639.

(20) Zhu, W.; Xu, M.; Chen, C. Z.; Guo, H.; Shen, M.; Hu, X.; Shinn, P.; Klumpp-Thomas, C.; Michael, S. G.; Zheng, W. Identification of SARS-CoV-2 3CL Protease Inhibitors by a Quantitative High-Throughput Screening. *ACS Pharmacol. Transl. Sci.* **2020**.

(21) Chen, L.-R.; Wang, Y.-C.; Lin, Y. W.; Chou, S.-Y.; Chen, S.-F.; Liu, L. T.; Wu, Y.-T.; Kuo, C.-J.; Chen, T. S.-S.; Juang, S.-H. Synthesis and evaluation of isatin derivatives as effective SARS coronavirus 3CL protease inhibitors. *Bioorg. Med. Chem. Lett.* **2005**, *15*, 3058-3062.

(22) Zhang, J.; Huitema, C.; Niu, C.; Yin, J.; James, M. N. G.; Eltis, L. D.; Vederas, J. C. Aryl methylene ketones and fluorinated methylene ketones as reversible inhibitors for severe acute respiratory syndrome (SARS) 3C-like proteinase. *Bioorg. Chem.* **2008**, *36*, 229-240.

(23) De Cesco, S.; Kurian, J.; Dufresne, C.; Mittermaier, A.; Moitessier, N. Covalent inhibitors design and discovery. *Eur. J. Med. Chem.* **2017**, *138*, 96-114.

(24) Zhou, S.; Chan, E.; Duan, W.; Huang, M.; Chen, Y. Z. Drug bioactivation, covalent binding to target proteins and toxicity relevance. *Drug Metab. Rev.* **2005**, 41-213.

(25) Guterman, L. Covalent Drugs Form Long-Lived Ties. *C&EN* **2011**, *89*, 19-26.

(26) Tang, B.; He, F.; Liu, D.; Fang, M.; Wu, Z.; Xu, D. AI-aided design of novel targeted covalent inhibitors against SARS-CoV-2. *bioRxiv* **2020**, 2020.2003.2003.972133.

(27) Nguyen, D. D.; Gao, K.; Chen, J.; Wang, R.; Wei, G.-W. Potentially highly potent drugs for 2019-nCoV. *bioRxiv* **2020**, 2020.2002.2005.936013.

(28) Roy, R.; Sk, M. F.; Jonniya, N. A.; Poddar, S.; Kar, P. Finding Potent Inhibitors Against SARS-CoV-2 Main Protease Through Virtual Screening, ADMET, and Molecular Dynamic Simulation Studies. . *ChemRxiv* **2020**, *Preprint*.

(29) Mariaule, G.; De Cesco, S.; Airaghi, F.; Kurian, J.; Schiavini, P.; Rocheleau, S.; Huskić, I.; Auclair, K.; Mittermaier, A.; Moitessier, N. 3-Oxo-hexahydro-1H-isoindole-4-carboxylic acid as a drug chiral bicyclic scaffold: structure-based design and preparation of conformationally constrained covalent and noncovalent prolyl oligopeptidase inhibitors. *J. Med. Chem.* **2016**, *59*, 4221–4234.

(30) Plescia, J.; Dufresne, C.; Janmamode, N.; Wahba, A. S.; Mittermaier, A. K.; Moitessier, N. Discovery of covalent prolyl oligopeptidase boronic ester inhibitors. *Eur. J. Med. Chem.* **2020**, *185*.

(31) Jacobs, J.; Grum-Tokars, V.; Zhou, Y.; Turlington, M.; Saldanha, S. A.; Chase, P.; Eggler, A.; Dawson, E. S.; Baez-Santos, Y. M.; Tomar, S.; Mielech, A. M.; Baker, S. C.; Lindsley, C. W.; Hodder, P.; Mesecar, A.; Stauffer, S. R. Discovery, Synthesis, And Structure-Based Optimization of a Series of N-(tert-Butyl)-2-(N-arylamido)-2-(pyridin-3-yl) Acetamides (ML188) as Potent Noncovalent Small Molecule Inhibitors of the Severe Acute Respiratory Syndrome Coronavirus (SARS-CoV) 3CL Protease. *J. Med. Chem.* **2013**, *56*, 534-546.

(32) Turlington, M.; Chun, A.; Tomar, S.; Eggler, A.; Grum-Tokars, V.; Jacobs, J.; Daniels, J. S.; Dawson, E.; Saldanha, A.; Chase, P.; Baez-Santos, Y. M.; Lindsley, C. W.; Hodder, P.; Mesecar, A. D.; Stauffer, S. R. Discovery of N-(benzo[1,2,3]triazol-1-yl)-N-(benzyl)acetamido)phenyl) carboxamides as severe acute respiratory syndrome coronavirus (SARS-CoV) 3CLpro inhibitors: Identification of ML300 and noncovalent nanomolar inhibitors with an induced-fit binding. *Bioorg. Med. Chem. Lett.* **2013**, *23*, 6172-6177.

(33) Moitessier, N.; Pottel, J.; Therrien, E.; Englebienne, P.; Liu, Z.; Tomberg, A.; Corbeil, C. R. Medicinal chemistry projects requiring imaginative structure-based drug design methods. *Acc. Chem. Res.* **2016**, *49*, 1646-1657.

(34) Behnke, D.; Taube, R.; Illgen, K.; Nerdinger, S.; Herdtweck, E. Substituted 2-(Cyanomethyl-amino)-acetamides by a Novel Three-Component Reaction. *Synlett* **2004**, *2004*, 688-692.

(35) Gedey, S.; Van der Eycken, J.; Fülöp, F. Liquid-Phase Combinatorial Synthesis of Alicyclic β-Lactams via Ugi Four-Component Reaction. *Org. Lett.* **2002**, *4*, 1967-1969.

(36) St John, S. E.; Mesecar, A. D. Broad spectrum non-covalent coronavirus protease inhibitors. USA Patent.

(37) Di Trani, J. M.; De Cesco, S.; O'Leary, R.; Plescia, J.; do Nascimento, C. J.; Moitessier, N.; Mittermaier, A. K. Rapid measurement of inhibitor binding kinetics by isothermal titration calorimetry. *Nat. Commun.* **2018**, *9*, 893.

(38) Zhang, L.; Lin, D.; Sun, X.; Curth, U.; Drosten, C.; Sauerhering, L.; Becker, S.; Rox, K.; Hilgenfeld, R. Crystal structure of SARS-CoV-2 main protease provides a basis for design of improved α-ketoamide inhibitors. *Science* **2020**, *368*, 409-412.

(39) Xue, X.; Yang, H.; Shen, W.; Zhao, Q.; Li, J.; Yang, K.; Chen, C.; Jin, Y.; Bartlam, M.; Rao, Z. Production of Authentic SARS-CoV Mpro with Enhanced Activity: Application as a Novel Tag-cleavage Endopeptidase for Protein Overproduction. *J. Mol. Biol.* **2007**, *366*, 965-975.

(40) Chen, S.; Chen, L.-l.; Luo, H.-b.; Sun, T.; Chen, J.; Ye, F.; Cai, J.-h.; Shen, J.-k.; Shen, X.; Jiang, H.-l. Enzymatic activity characterization of SARS coronavirus 3C-like protease by fluorescence resonance energy transfer technique. *Acta Pharmacol. Sin.* **2005**, *26*, 99-106.